Development of Pick-and-Place Assembly Techniques for Monolithic Optopill Integration

by

Mindy Simin Teo

B.S.E. Electrical Engineering
University of Michigan, Ann Arbor 2003

Submitted to the Department of Electrical Engineering and Computer Science in Partial Fulfillment of the Requirements for the Degree of

Masters of Science in Electrical Engineering

at the

Massachusetts Institute of Technology

January 2005

Signature of Author: _____

Department of Electrical Engineering and Computer Science
January 16, 2005

Certified by: _____

Clifton G. Fonstad, Jr.
Vitesse Professor of Electrical Engineering
Thesis Supervisor

Accepted by: _____

Arthur C. Smith
Chairman, Department Committee on Graduate Students

Development of Pick-and-Place Assembly Techniques for Monolithic Optopill Integration

by

Mindy Simin Teo

Submitted to the Department of Electrical Engineering and Computer Science
on January 16, 2004 in Partial Fulfillment of the
Requirements for the Degree of Master of Science in
Electrical Engineering

ABSTRACT

The monolithic heterogeneous integration technology known as Recess Mounting with Monolithic Metallization (RM^3) has been under study to integrate III-V heterostructures in the form of optopills on silicon CMOS circuits. Implementation of this technology poses several challenges such as recess filling and optopill bonding to the CMOS circuits. Research focused on establishing assembly techniques to overcome these challenges is performed. This thesis discusses the development of a vacuum tool pick-and-place technique as a solution to recess filling. A novel vacuum film bonding technique was also studied as a method of bonding the pills to the recesses. The results of this bonding technique as well as bonding experiments done using various metal stacks between the pills and recesses are also presented here.

Thesis Supervisor: Clifton G. Fonstad, Jr.
Title: Vitesse Professor of Electrical Engineering

Acknowledgements

I owe a multitude of thanks to the many people who have given me the much needed guidance and support toward writing this thesis. The first people I must thank are my parents, who have been a constant source of good advice and moral support. To the rest of the family, Ngor Yee Yee, Uncle Malcolm, Poh Poh, Uncle Chu, Kuan Yee Yee, Kou Fu and Kou Mo, thank you for your regular phone calls from Singapore and Canada that have kept me out of bouts of homesickness.

A great debt of gratitude is also owed to my scholarship company, Singapore Technologies Pte. Ltd., for sponsoring the most part of my tertiary education. My scholarship officer and the HR director, Noreen and Irene, have been more than just scholarship administrators to me. Thank you for being so supportive and encouraging me to widen my horizons over the past 5 years.

Prof. Fonstad, who has been so kind, understanding and patient, has been a wonderful thesis supervisor. I must thank him for his guidance and invaluable input to my research.

The members of Prof. Fonstad's group have also helped me in various ways. James Perkins and Joe Rumpler, have given me much assistance especially since they fabricated all the optopills that I've been using. Thanks as well for being the resident jokesters of our group! Henry Choy has shown me the ropes and given me great advice, be it how to order a tank of gas or ideas on bonding experiments. I could not ask for a better officemate. Thank you! I have to thank Wojciech for providing me much needed assistance with using various pieces of lab equipment. I really appreciate Vivian's efforts in helping me settle comfortably into graduate school as well as the environment at MTL. Ed Barkley has always been a friendly face along the third floor corridor of building 13 and helped me feel welcome. Of course, I must also thank Prof. Sheila Prasad for always having kind words to say to me.

I owe many thanks to Kurt Broderick for training me to use the equipment in EML and helping me whenever I had problems during processing. Dan Adams has also been a

great help with the die saw. I really appreciate the extra effort to help me with drilling and cutting that piece of ceramic I needed for my bonding set up. I would also like to thank Patrick Boisvert for his patience and help on using the SEM in the CMSE-SEF. In addition, I must thank Paul Tierney, Bob Bicchieri, and Jim Daley for training me to use various machines in TRL and NSL. Peter Morley has also been wonderful in helping me get parts machined for the bonding set-up.

I would also like to thank April Dean from Precision Micro Devices, as she has been most helpful with giving me ideas on using the micropipettes.

Without the support of my friends, this thesis would not have been possible either. They have helped me maintain a healthy lifestyle and find a balance between work and play. I must thank Trina for her precious friendship and lovely visits over the past few years, as well as Lindsay, Yiling, Hin Meng and Trevor for keeping me company on our weekend endeavors outside the confines of graduate school. Last but not least, Tzu Liang has been my pillar of support (and a source of exasperation at times) over the past 4 years, and has helped me get through numerous crises. I sincerely thank him for putting up with my stress attacks and eccentricities and being a wonderful housemate and going with me to those yoga classes against his will.

Contents

List of Figures

List of Tables

Chapter 1

Introduction

1.1. Motivation for Monolithic Optoelectronic Integration

Heterostructure III-V optical devices such as laser diodes and p-i-n detectors are already widely used as fundamental components of common items like fiber communication systems, cellular telephones, and compact disk players. The optoelectronic properties of III-V materials such as indium phosphide (InP) and gallium arsenide (GaAs) are superior to those of silicon. Most III-V materials are direct bandgap and thus electrons in them can make highly efficient optical transitions. Moreover, the physical and chemical III-V material properties can be tuned over a large range to adjust the bandgap, thus providing great flexibility. Using advanced deposition techniques like Molecular Beam Epitaxy (MBE), high quality, low defect III-V material can be grown with the desired bandgap profiles.

Conversely, silicon has an indirect bandgap that results in weak emission and absorption of light, as energy transitions require both photons and phonons. Such multi-particle interactions have a low probability of occurrence compared to the direct electron transitions in direct bandgap materials. This low quantum efficiency renders silicon impractical for optoelectronic applications such as laser diodes.

Nevertheless, while silicon is an unsuitable material for optoelectronic devices, it is an ideal platform for heterogeneous integration with III-V heterostructure devices. This is largely due to the existence of an established, mature high performance integrated circuit technology for silicon. This means that high quality silicon and silicon-on-insulator (SOI)

materials are relatively inexpensive to produce in large wafer diameters that ensure a high number of chips per wafer. Moreover, silicon is a better heat-conducting platform than compound semiconductors, and thus may ensure greater power efficiency of devices like lasers and power transistors. Integrating III-V heterostructures onto commercially processed high density Si integrated circuits, such as VLSI and ULSI circuits, thus enables us to reap the benefits of both III-V optoelectronic functionality and the established Si process technology.

For instance, optical interconnections in an optoelectronic integrated circuit (OEIC) can overcome the limitations otherwise imposed by electrical interconnections on the density and speed of integrated circuits, such as high levels of power dissipation and large wire parasitics. This could also increase the available bandwidth of the system and reduce the susceptibility to electromagnetic interference.

However, a technology capable of compact and efficient heterogeneous optoelectronic integration is desired to maximize the potential advantages of such integration.

There are two classifications of optoelectronic integration technology, namely hybrid integration and monolithic integration. Hybrid integration generally consists of integrating III-V optical device circuits and fully processed Si CMOS integrated circuits (ICs) on the same substrate or package. There are several methods, such as wire bonding, to interconnect the distinct chip-level components. Flip-chip bonding and selective thinning of the heterostructure devices are some of the other implementations of hybrid integration technology that have been demonstrated. For instance, vertical-cavity surface-emitting lasers (VCSEL's) have been successfully bonded to high performance CMOS circuits [1] and high electron mobility transistors (HEMT's) selectively thinned for integration without much decrease in device performance [2].

Hybrid integration offers an immediate and relatively simple solution to manufacturing OEIC's while providing some space and package savings and allows for testing of the discrete components before assembly. However, hybrid integration does not allow for the high device densities that are required for high performance OEIC's. Due to

the discrete, chip-by-chip nature of such integration, there is minimal cost saving as the labor-intensive manufacturing, testing and interfacing of individual chips does not provide for economies of scale. The processing costs are further heightened by the need for precise alignment when interconnecting individual components, and device complexity and reliability are compromised due to problems like interfacing losses and reflections.

Monolithic integration, on the other hand, refers to the integration of all optoelectronic components on a single chip. Combining all required functionalities on a single unit ensures higher device density and reduced circuit size. Monolithic integration can accommodate higher circuit complexity and promises better system reliability, as the need for alignment sensitive inter-chip connections is eliminated. There is also the advantage of reduced per unit cost, as mass production is possible since the integrated devices can be batch processed on large Si wafers. Hence, in the long run, monolithic integration offers a more cost-effective, scaleable, and therefore practical solution to optoelectronic integration, as compared to hybrid integration.

Material	**Lattice Constant (Å) at 25°C**	**Coefficient of Thermal Expansion (10^{-6}/°C) at 300K**
Si	5.4309	2.6
InP	5.8687	4.75
GaAs	5.6532	6.86

Table 1-1 Material Properties of Si, InP and GaAs [3], [4]

Nevertheless, implementing monolithic integration is not without its challenges. The key obstacles faced by optoelectronic integration are the lattice and thermal expansion mismatch between III-V semiconductors and silicon. Table 1-1 illustrates this mismatch. Traditional approaches to monolithic integration, which usually use direct epitaxy of III-V material on Si substrates, are therefore hindered. This is because the mismatch in the crystallographic structures causes stress in the epitaxial growth, resulting in defects and compromising the quality of the heterostructure device. While the lattice mismatch can be overcome by special techniques such as intermediate buffer layers, the thermal expansion mismatch is a bigger problem [5]. Due to the large difference in the Si and III-V material thermal expansion coefficients, a significant number of defects are

introduced when the grown structures are cooled from growth temperatures to room temperature. The material quality and thus device performance is severely limited by such defects.

Therefore, alternative monolithic integration technologies must be developed to ensure that this mode of integration becomes a viable long term solution to optoelectronic integration applications.

1.2. Current Integration Technologies

Various heterogeneous optoelectronic integration techniques have been developed. To provide a better perspective of the progress of optoelectronic integration, some of these techniques are described in this section, along with their advantages and limitations.

1.2.1. Flip Chip Bonding

Flip chip bonding is one of the commercial approaches to hybrid integration. There are several flip chip bonding techniques, such as solder bump flip chip bonding and plate bump flip chip bonding but the general concept remains the same. Conductive bumps are deposited on the bond pads on the device chips to provide an electrical, thermal and mechanical connection between the device die and the substrate IC. The bumps also serve as a spacer between the device die and substrate IC. Solder is then deposited on the bumps. The die is then flipped and aligned face down onto the substrate IC. Static pressure and heat are applied to enable bonding. A non-conductive underfill adhesive is commonly applied between the two bonded chips to improve mechanical strength. Figure 1-1 shows the cross section of a flip-chip bonded device that has epoxy wicked between the two dies to serve as the underfill [1].

Flip chip bonding promises good electrical performance, mechanical robustness, reliability, and also has the advantage of self-alignment. It is more efficient, and has reduced interconnect parasitic effects, compared with wire bonding, another hybrid integration technique [6]. However, it can only be used for integration on a chip-by-chip basis (as opposed to entire wafers) and cannot support batch processing of high density devices, which is desirable for large-scale integration.

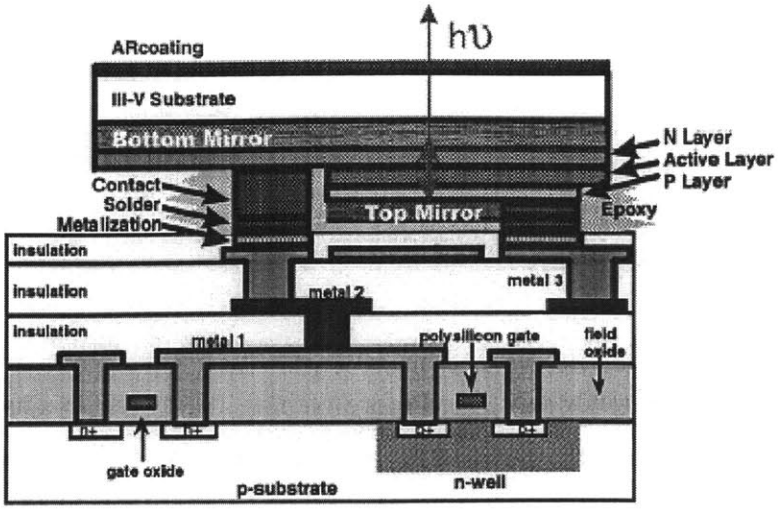

Figure 1-1 Schematic of III-V VCSEL flip-chip bonded to Si CMOS circuit. [1]

1.2.2. Wafer Bonding

Wafer bonding utilizes the van der Waals bonds between two highly planarized semiconductor materials or a semiconductor and an insulator, as opposed to the metal-to-metal bonds used in flip chip bonding, to bond two processed wafers. Elevated temperatures (300°C-500°C) and even pressure may be applied to facilitate bond formation. Usually, one of the wafers is subsequently thinned down to remove the original III-V growth substrate and to allow for through-wafer electrical connections [7].

Unlike flip chip bonding, this technique supports wafer-scale integration. However, this advantage is limited by the small III-V material wafer sizes (150 nm for GaAs and 100 nm for InP). The small wafer size is attributed to the brittleness of the compound semiconductors. Wafer bonding is also plagued by the problem of material mismatch. Due to the high temperatures involved in wafer bonding, the mismatch of the thermal expansion coefficients of Si and III-V materials can result in bond failure due to the high stress at the bond interface [8].

1.2.3. Direct Epitaxy

This monolithic technique involves direct epitaxial growth of III-V materials on a silicon substrate using molecular beam epitaxy (MBE) or similar methods. Interfacial stress and strains, due to the material property mismatches cited earlier, lead to reduced

lifetimes and severely affect device performance. Although growing a thick strain relief layer or using buffer layers may alleviate some of these problems, there still remains the need to maintain low growth temperatures [9]. Temperatures of subsequent processing steps are also limited.

1.2.4. Fluidic Self Assembly (FSA)

This is a monolithic integration technique which entails processing devices separately on their growth substrate before etching them free to form "blocks". These blocks correspond to the receptor sites that are etched in the target substrates. The blocks are then suspended in a fluid which is then pumped repeatedly over the target substrate, where the blocks fall into the receptor sites. Blocks that miss the receptor sites are re-circulated and flowed over the target substrate again until the receptor sites are filled [10]. The blocks are bonded to the receptor sites, and the filled target substrate is then planarized and processed monolithically. This technique has almost 100 % yields for large blocks (> 150 μm on a side), but has limited yields for smaller blocks [11].

1.3. Thesis Organization

This thesis describes the development of the microscale pick-and-place (MPAP) and vacuum film bonding techniques. These techniques are potential solutions to the implementation of an alternative monolithic integration technology, Recess Mounting with Monolithic Metallization (RM^3).

Chapter 2 describes the RM^3 techniques that have or are being studied. The advantages of Optopill assembly (OPA) and the concept of MPAP are also discussed. The results of the study on MPAP are presented in Chapter 3. Chapter 4 describes the development of a vacuum film, high pressure bonding system for bonding the optopills to pads in the recesses. The justification for various metal bonding stacks used for this purpose and the experimental results of these bonding studies are presented in Chapter 5. Conclusions on the development of MPAP and bonding techniques as well as a discussion of future research possibilities are included in Chapter 6.

1.4. Lab Facilities

The microscale pick and place procedures, bonding experiments and some metal deposition were carried out in Prof. Fonstad's electronics and processing labs respectively. Most of the other fabrication processes were done in the Microsystems Technology Laboratories (MTL), specifically in the Exploratory Materials Laboratory (EML). All SEM images were taken using the Environmental Scanning Electron Microscope (ESEM) in the MIT-Center for Material Science and Engineering (CMSE) Electron Microscopy Shared Experimental Facility (SEF).

Chapter 2

A New Concept --- Microscale Pick-and-Place Assembly (MPAP)

2.1. Recess Mounting with Monolithic Metallization (RM^3)

Recess mounting with monolithic metallization (RM^3) has been proposed as a means of interfacing optical and electronic device capabilities compactly and efficiently. This integration technology accommodates III-V heterostructures in recesses etched in commercially processed chips such as Si-CMOS VLSI circuits. These heterostructures are either grown in the recesses, or grown on a separate substrate prior to being positioned in the recesses and subsequently bonded to the IC chips. These recesses are dielectric windows on the IC chips. Subsequently, the chips are processed monolithically to complete the optoelectronic device integration. Figure 2-1 provides a visual of this process. One of the key challenges posed by the implementation of RM^3 is filling the recesses. Previously studied implementations of this technology and their limitations are discussed below.

2.1.1. Previously Investigated Implementations of RM^3

Previously studied methods of filling the recesses are Epitaxy-on-Electronics (EoE) and Aligned Pillar Bonding (APB). The EoE technique involves growing III-V heterostructures epitaxially in recesses where the substrate surface in selected areas on fully-processed GaAs integrated circuit wafers are exposed [12]. APB, on the other hand, uses aligned, selective-area bonding to integrate heterostructures onto processed IC

wafers. The heterostructures are grown on an optimal substrate wafer using molecular beam epitaxy (MBE), patterned into pillars, then bonded into recesses on the target IC wafer using either fusion or metallurgical bonding. The substrate wafer is then removed by etching. The EoE and APB techniques are described in Figures 2-2 and 2-3 respectively.

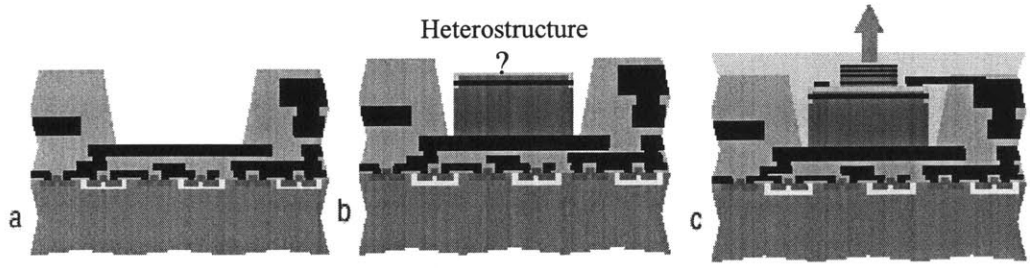

Figure 2-1 Schematic of a RM^3 Process: a) Recess etched in commercially processed IC wafer and contact-cum-bonding pads deposited in recesses. b) Device heterostructure placed or grown in recess. c) Assembled circuits are processed monolithically.

One of the key limitations of EoE is that it is only compatible with IC wafers of the same composition as the heterostructures grown on the IC wafers. This is due to the issues of lattice constant and thermal expansion coefficient mismatch that compromise device performance if the IC substrate and heterostructure are of different material composition. EoE is thus less versatile and cannot be applied to Si IC wafers effectively. Moreover, due to the need for a thorough cleaning process when opening the growth recesses to ensure good quality growth, yields are relatively low over the entire die. In addition, the MBE growth temperature is limited to below 475 °C to prevent chip damage [13].

Conversely, APB is compatible with a wider range of IC wafer and alleviates the problems due to thermal expansion coefficient mismatch. This is because the heterostructures and Si circuits are grown or processed optimally on separate substrates. However, it does not allow for efficient use of the epitaxial material, as much of this is etched off during the patterning to form the pillars.

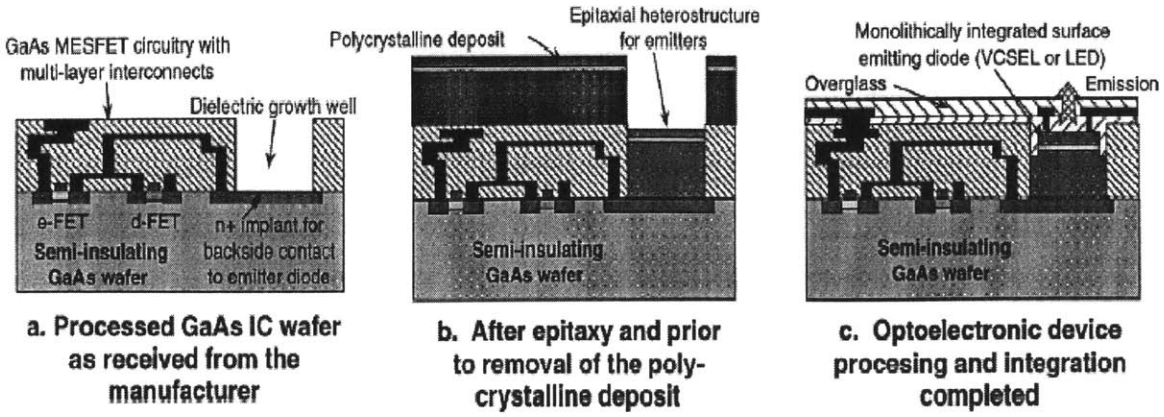

Figure 2-2 Illustration of EoE technique. [14]

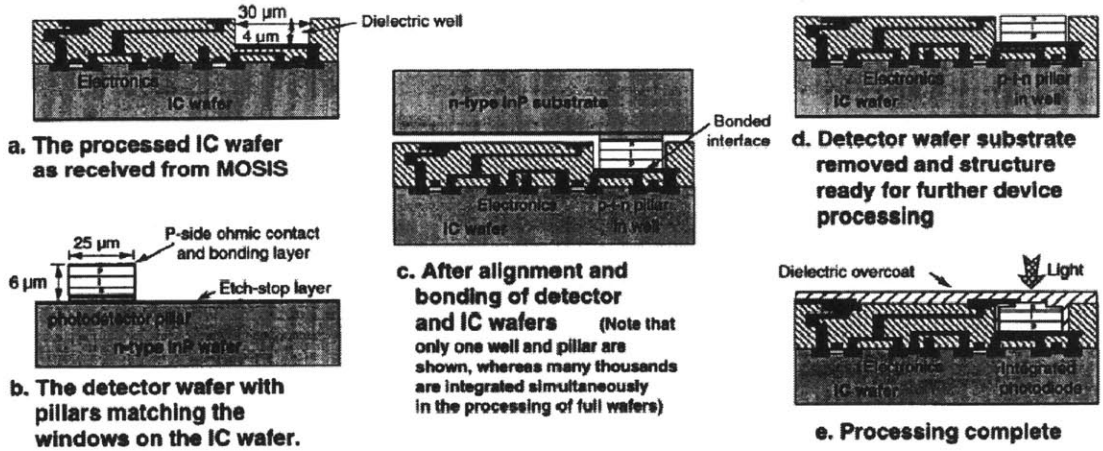

Figure 2-3 Illustration of APB technique. [14]

2.2. Introduction to Microscale Pick-and-Place (MPAP)

The microscale-pick-and-place (MPAP) technique is proposed as an RM^3 solution to filling the recesses. This technique seeks to overcome the limitations imposed by EoE and APB on monolithic integration. MPAP is an OptoPill Assembly (OPA) technique used to pick up III-V heterostructure devices in the form of optopills and place them in strategically located recesses on target substrates. Target substrates refer to the IC chips or wafers on which the optoelectronic devices are to be integrated.

The idea of MPAP is to start with developing a manually controlled pick-and-place method first, before refining it into an automated pick-and-place technique that will increase the assembly efficiency manifold. Thus, while MPAP may seem unattractive initially due to its pill-by-pill approach, the potential for mechanization of the process

should be taken into consideration. Further advantages of MPAP are discussed later in this chapter.

Another OPA technique that is concurrently being studied is Magnetically Assisted Statistical Assembly (MASA) [15], [16]. This technique utilizes attractive magnetic forces to assemble the pills in the recesses and will not be discussed further. The optopills used in MPAP and MASA are fabricated using the same process.

The two main steps involved in MPAP, namely optopill fabrication and pick-and-place assembly, are described briefly as follows.

2.2.1. Optopill Fabrication

The optopill fabrication entails growing the heterostructures on a suitable device substrate. The heterostructure material is optimally processed on its growth substrate before being patterned into cylindrical pillars. These cylindrical pillars are termed "optopills". This optopill fabrication process has been developed by J. Rumpler and J. Perkins [15], [16].

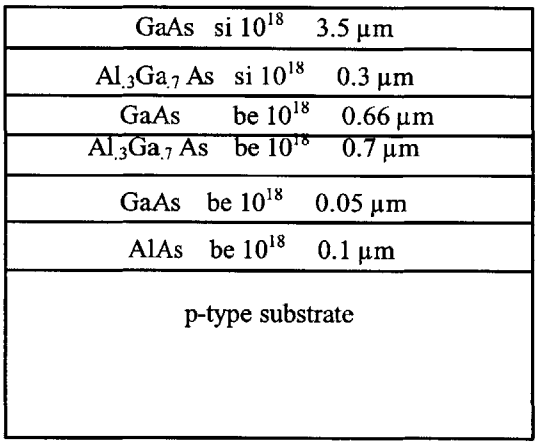

Figure 2-4 Sample optopill structure (not to scale): an LED grown bottom-side up on p-type substrate. The AlAs layer is a sacrificial layer, and the AlGaAs layers serve as confining regions on both sides of the GaAs active layer.

Typically, the optopills are MBE grown, bottom-side up, with a sacrificial layer grown between the actual device and the growth substrate. This layer facilitates etching the optopills free of their substrate. The optopills are then collected on an adhesive such

as a polymer, and placed in a fluid such as a solvent to dissolve the adhesive. The pills in the solution are then dispensed on a flat substrate to be picked up and assembled by MPAP into their target recesses on integrated circuit wafers. Figure 2-4 is an example of an optopill structure described in [16].

2.2.2. Pick-and-Place Assembly of Optopill in Recesses

This step involves manipulating a narrow tipped tool of the order of 20-60 μm in diameter to pick up similarly sized optopills that have been dispensed onto a flat substrate, and place them in their target recesses, as shown by Figure 2-5.

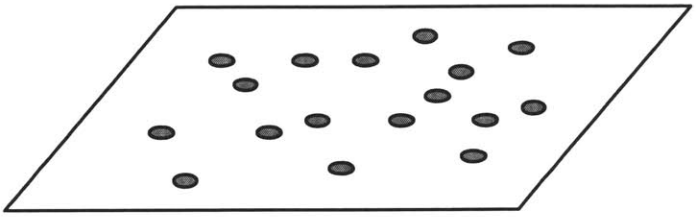

a) Optopills dispensed on flat substrate e.g. glass slide

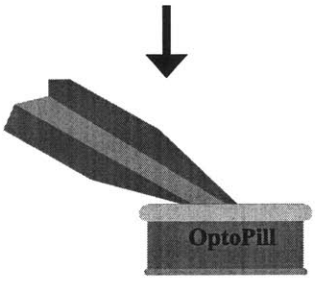

b) OptoPill picked up by narrow tipped tool

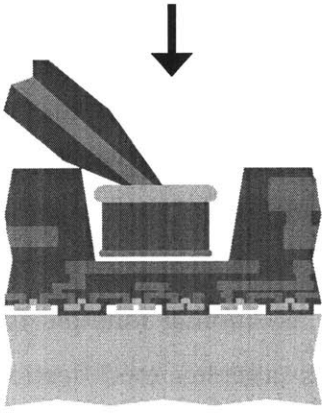

c) Optopill placed in recess on target substrate using narrow tipped tool

Figure 2-5 Schematic of the MPAP technique.

Two methods of MPAP have been investigated. Both use a micro-manipulator to control the pick-up tool. The first uses a metal probe tip coated with a thin film of liquid to pick up the pills and place them accordingly. The second requires the use a vacuum pick-up tool to assemble the pills. Both techniques will be discussed in detail in the next chapter.

After the optopills are assembled, they are bonded to metallurgical pads in the recesses on the target wafers. The bonded pills and the target wafers are then processed monolithically.

2.3. Benefits of MPAP

MPAP is a promising monolithic integration technique due to a number of advantages that it has to offer. Firstly, as the heterostructure devices are grown on a separate substrate, they can be grown under optimal conditions on optimum substrates, ensuring high quality device performance. The MBE growth temperature is not limited by chip tolerances, unlike EoE.

Having a separate device growth substrate means that the target IC substrate wafer size is not restricted by the wafer size typical of the heterostructure material. This enables the use of standard wafer sizes, and is especially advantageous when integrating III-V materials onto Si target ICs, since III-V wafers are typically much smaller than Si wafers.

MPAP also provides a greater degree of flexibility, as the optopill structure and material can be varied depending on the heterostructure device functionality required. MPAP can thus be applied to a wide range of optoelectronic integration needs.

Multiple types of heterostructure devices can also be assembled on a single target IC substrate using MPAP, since each type of device can be grown and processed into optopills on separate growth substrates before being integrated. With techniques like MASA and APB, however, assembling multiple types of heterostructures on a single substrate will be difficult as complex modifications have to be made. For instance, performing such integration using MASA may require variation in the shape of the optopills and recesses to ensure the right heterostructure device falls in each target recess.

Conversely, no modification to the MPAP technique is required to accommodate this mode of integration. MPAP is thus highly practical for complex optoelectronic designs where more than one type of heterostructure device is desired, as compared to other RM^3 techniques.

In addition, the heterostructures can be grown in a densely packed pattern that ensures efficient use of the epitaxial material. While the cylindrical pills are producible in many material systems due to their symmetry, pills of other shapes can also be fabricated using different mask patterns. For instance, square or rectangular p-i-n diode pills may be grown to interface with waveguides. This adds to the versatility of the MPAP technique.

Moreover, MPAP can be used to place heterostructure devices atop existing devices on the target substrate, enabling 3-D circuit capacity. The optopills can also be tested before integration to ensure that working devices are assembled on the target substrate [16].

Although MPAP may seem tedious, it lays the foundation for future mechanized methods of pill assembly. If adapted into an automated assembly technique of a reasonable efficiency, it may be compatible with wafer batch processing. Thus MPAP is a novel integration technique worth looking into.

Chapter 3

Development of MPAP

The two MPAP techniques that have been developed will be discussed in this chapter. This study utilized similar optopills to develop both techniques. The optopills used had a thickness of 5 – 6 μm and were 35-50 μm in diameter. For this study, the actual composition of the III-V optopills was not as important as the size and shape of the pill. Thus, some of the optopills used had a structure similar to that described in Figure 3-1. These dummy optopills had no actual device functionality but were sufficient for determining the practicality of MPAP. The metal layers were varied depending on the bonding experiments that were conducted using the placed pills. More detail regarding this will be given in Chapters 4 and 5.

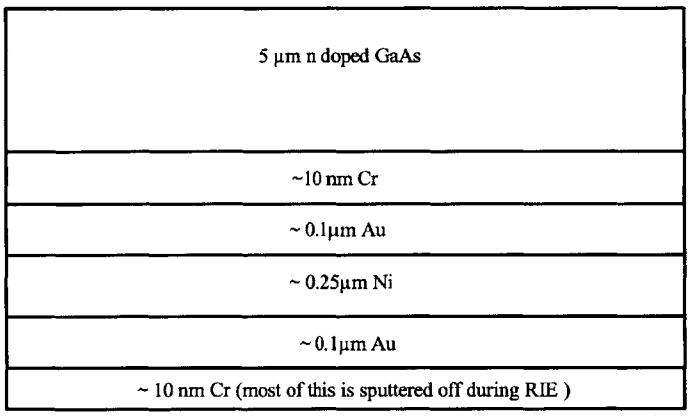

Figure 3-1 Schematic of typical dummy optopill used in MPAP study (not to scale): The pill here is right side up. The probe tip or vacuum tool contacts the exposed surface of the GaAs layer. The layer of Cr directly in contact with GaAs serves as an adhesion layer for the next Au layer, which is used for ohmic contact. The magnetic Ni layer enables the pill to be used for MASA as well. The bottom Au layer is used for bonding to AuSn pads. The bottom most Cr layer was to promote oxide mask adhesion for a pill processing step, and most of it is sputtered off during reactive ion etching (RIE) to remove the oxide mask.

These optopills were collected as described in [15], [16], and subsequently dispensed in methanol on either glass slides or pieces of polished Si for MPAP. The optopill fabrication, collection and dispensing were done by J. Perkins and J. Rumpler. Figure 3-2 shows some of these pills that have been dispensed on a glass slide. About 50 to 100 pills were dispensed each time. The pills were picked up by either MPAP method and placed on both flat substrates and recesses etched into substrates like Si or silicon dioxide.

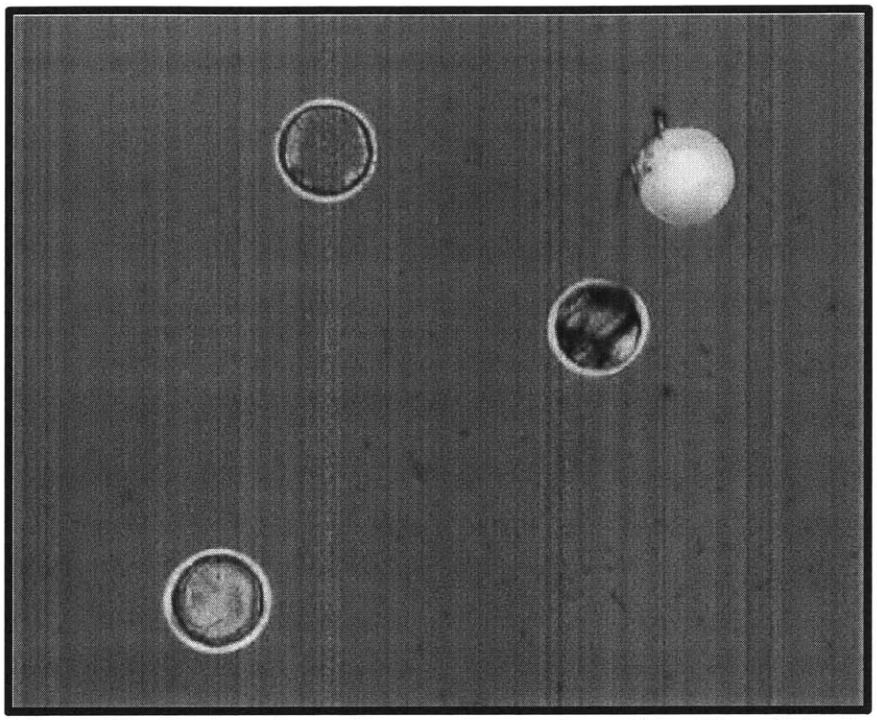

Figure 3-2 Optopills that have been dispensed on a glass slide: The pill in the top right corner is bottom side up, with the metal layer facing up, and thus will not be used for MPAP. The rest of the pills in this image are right side up, and thus suitable for MPAP. The semiconductor layer is 35 μm in diameter while the metal pad is 45μm in diameter. This discrepancy is due to over-etching of the semiconductor layer. This discrepancy is evident in the two "rings" seen on the right-side up pills.

3.1. Probe Tip MPAP

It was initially observed that a dirty probe tip, when placed on the top surface of an optopill, could be lifted up with the optopill still attached to the probe tip. Thus it was inferred that using either static force or adhesive force, it would be possible to pick-and-place optopills using a probe tip.

The probe tips used had a tip diameter of approximately 10 μm. The fine tip diameter ensured the probe tip did not obscure the optopill and allowed for a good view of the pill during pick-and-place. Before using any probe tip to pick up optopills, it was cleaned with isopropanol. To enable controlled manipulation of the probe tip, the cleaned probe tip was attached to a micromanipulator like those commonly found on manual probe stations.

Using a microscope for visual aid, the probe tip was maneuvered over the glass slide or flat substrate of pills and carefully positioned directly above an optopill. It was then lowered to come into contact with the top surface of a dispensed optopill. Only optopills that were oriented right-side up were selected. This is illustrated in Figure 3-3. A right-side up pill refers to a pill where the metal layers are facing down and in contact with the glass slide or flat substrate, and the semiconductor layer is the top, exposed layer (i.e. the probe tip contacts the semiconductor layer). The pills that were wrong-side up could be rinsed off the flat substrate, recollected in solvent and dispensed again for MPAP to minimize pill wastage.

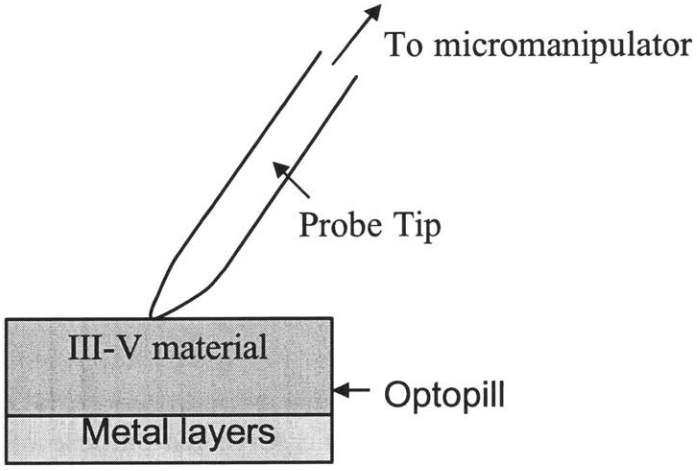

Figure 3-3 Diagram showing how a probe tip is used to pick up an optopill.

The probe tip was slightly lowered so some pressure was applied on the pill before it was lifted up again. This was repeated until the pill was picked up and attached to the probe tip. The probe tip, with the pill attached, was then moved and lowered onto the target substrate or recess until the bottom surface of the pill was in contact with the target pad. The static forces between the bottom of the pill and the target pad sometimes

overcame the adhesive forces between the pill and the probe tip, enabling pill placement. The probe tip could also be lightly moved around to loosen the pill onto the flat substrate or into the recess. If this did not work, another cleaned probe tip was used to nudge the pill off the tip and onto the target pad.

3.1.1. Investigation of Suitable Adhesive Film for Probe Tip MPAP

It was first attempted to use clean probe tips to pick up and place pills using sheer static force. However, this method failed, as the dispensed pills would not adhere to the probe tip and could not be lifted up from both the glass slide and polished Si surfaces. The only way that a pill could be picked up was when the probe tip had dust or dirt on it. This dirt was visible under the microscope. Such levels of contamination would definitely affect any post-assembly processing.

It was therefore concluded that relying on static force alone for MPAP was insufficient, and it would be necessary to apply an adhesive film on the probe tip to aid in pill pick up. It was preferable that this film could be easily removed after pill placement. Several liquids were considered as it was thought that coating a probe tip with a thin film of liquid would provide sufficient adhesive force between the tip and the optopills. A cleaned probe tip was coated with the desired liquid film by dipping it in the respective liquid before being used to pick up the optopills. The liquids tested and the results are discussed in the following subsections. Each liquid was used in at least twenty attempts to pick up pills.

3.1.1.1. Deionized Water

It was hoped that deionized water would serve the purpose of an adhesive film. This was because of its neutral properties and that any deionized water on the top surface of the optopill could be easily removed by a simple evaporation step with little effect on the optopill or the underlying circuitry the pill was placed on. Unfortunately, repeated attempts to pick up optopills using probe tips dipped in deionized water were unsuccessful. The only time a pill could be picked up, after several tries (i.e. the probe tip was lowered into contact with the pill and raised up repeatedly), occurred when an entire

drop of water was dripped on the glass slide, wetting all the pills in the area of the water drop. This was not an option for MPAP, as it was not desirable to coat the entire pill in deionized water, and removing liquid between the bottom side of the pill and the pad in the target recess would be a problem.

It was inferred that perhaps a more viscous liquid would provide better adhesive force than deionized water. Two such liquids, photoresist and glycerol, were tested.

3.1.1.2. Photoresist

Two types of photoresist were experimented with under the consideration that photoresist could be easily removed by acetone after MPAP. The first was the thick resist AZ 4620, and the latter was AZ 5214 which is typically used for image reversal photolithography. AZ 4620 was too thick, and messy blobs of resist tended to form on the probe tips, rendering impossible to get a good view of the pills underneath the tips. Conversely, the less viscous AZ 5214 did not provide sufficient adhesive force for the pills to stick to the probe tips.

3.1.1.3. Glycerol

Glycerol was also too viscous and had a tendency to clump up. The surface tensional forces within the glycerol drops were far stronger than the adhesive forces between the pills and the glycerol. Thus the pills could not be picked up effectively. Moreover, there is no easy way to remove glycerol as it is not vaporizable.

It was therefore found that thick, viscous liquids were unsuitable for probe tip MPAP. Water soluble adhesive and two less viscous liquids were tested next.

3.1.1.4. Water Soluble Adhesive

Water soluble adhesive from water soluble tape was transferred onto the probe tip by wiping the tape on the probe tip. It was very easy to pick up the pills as the soluble adhesive provided a strong adhesive force between the pill and the probe tip. However, it was almost impossible to remove a pill from the tip and onto the target substrate or recess

once the pill was stuck to the probe tip. Using a second probe to knock the pills off the first probe and onto the recess did not work effectively either.

3.1.1.5. Pump Oil

Pump oil was used rather successfully as an adhesive film on the probe tips to pick up the optopills. An experiment was done to get an idea of the effectiveness of pump oil as an adhesive film. Attempts were made to pick up 50 optopills from a glass slide using pump oil coated probe tips. Out of the 50 optopills, 27, or 54% of pills were successfully picked up within 2 tries. The rest of the pills were broken during the attempts to pick them up when too much pressure was applied on them via lowering the probe tip.

In fact, the pills adhered so well to the probe tip that it was difficult to place them on either flat substrates or in recesses etched in a piece of Si. A second, uncoated probe tip attached to another micromanipulator had to be used to nudge the pills off the pump oil coated probe tip and onto the target pads. This is demonstrated in Figure 3-4.

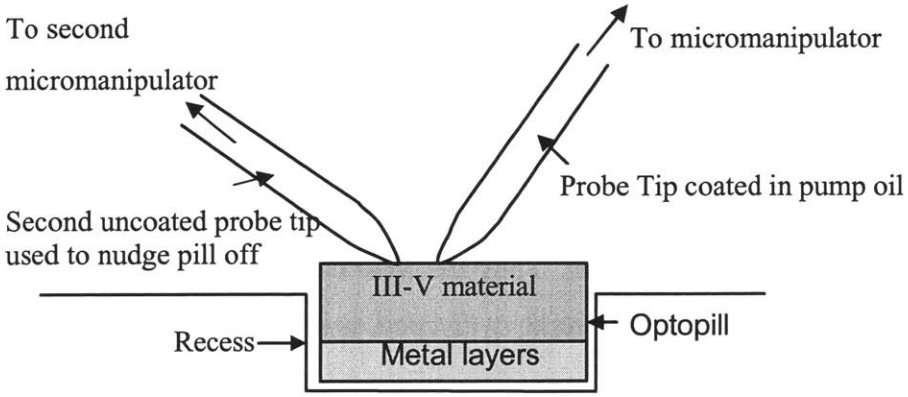

Figure 3-4 Schematic of how second probe tip is used to nudge optopill off into recess.

However, pump oil is not easily removed, as it cannot be evaporated away. A degreaser could be used to remove the pump oil, but this would require an elaborate set-up and it would be difficult to ensure that the pills stayed in place on the target substrates during degreasing. Moreover, degreasing will involve condensation of the solvent used in the vapor degreaser on the entire chip surface.

3.1.1.6. Solder Flux

An alternative was sought in solder flux. SuperSafe Superior No. 30 liquid solder flux was used. It was found that solder flux was a more effective pick-up adhesive film than the pump oil. While a second probe tip was also needed to assist in placing the pill, less liquid residue was left behind on the top surface of the pill after pill placement. Figure 3-5 shows a pill that had been placed successfully in a recess using solder flux assisted probe tip MPAP. In addition, solder flux becomes completely neutral, electrically non-conductive and non-hygroscopic upon heating properly, and can thus be removed by evaporation.

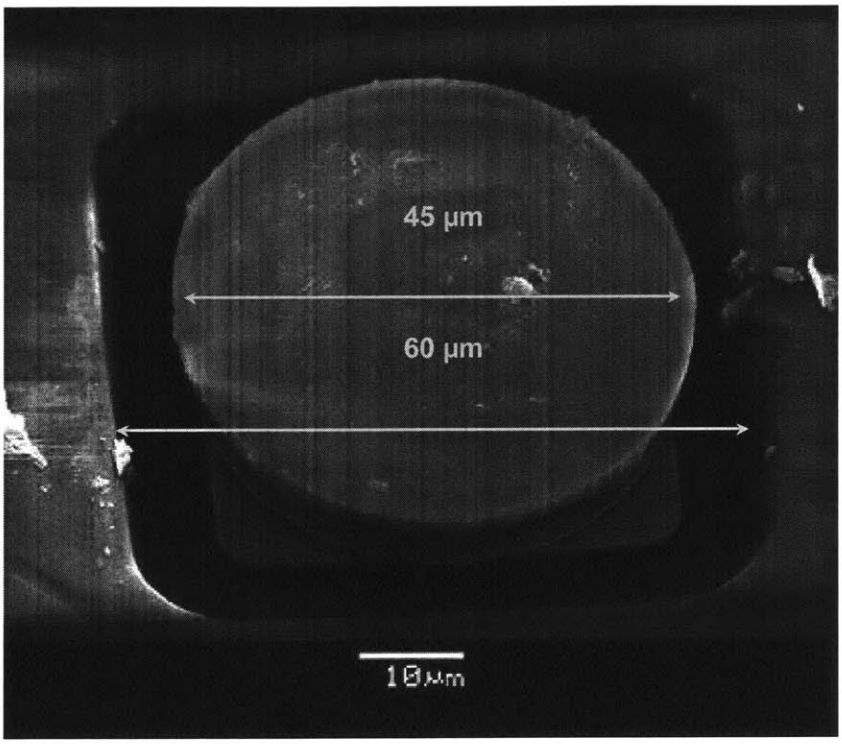

Figure 3-5 Image of optopill placed in a square recess on a silicon CMOS IC chip using solder flux assisted probe tip MPAP.

Although solder flux provided a relatively cleaner probe tip MPAP solution, there was still concern that some residue would be left behind after evaporating most of the solder flux and an additional step would be required to remove this residue. Moreover, there was a strong tendency for the pills to break during attempts to pick them up. This was due to the pressure that had to be applied by the probe tip for the pill to adhere. A cleaner MPAP process with a more effective mode of pill pick-up was desired.

3.2. Vacuum Tool MPAP

The second technique investigated uses micropipettes with pulled tips as a vacuum pick-up tool in place of the probe tip. These micropipettes are not unlike those used in biological applications such as cell biology. A clean micropipette is attached to a micropipette holder that is connected to a micromanipulator for controlled maneuvering of the micropipettes. This part of the set-up is shown in Figure 3-6.

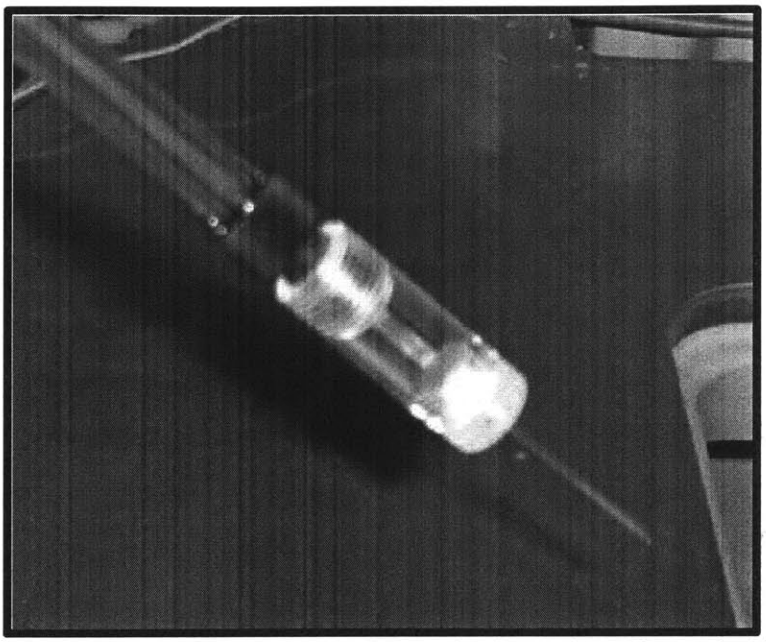

Figure 3-6 Image of micropipette attached to micropipette holder.

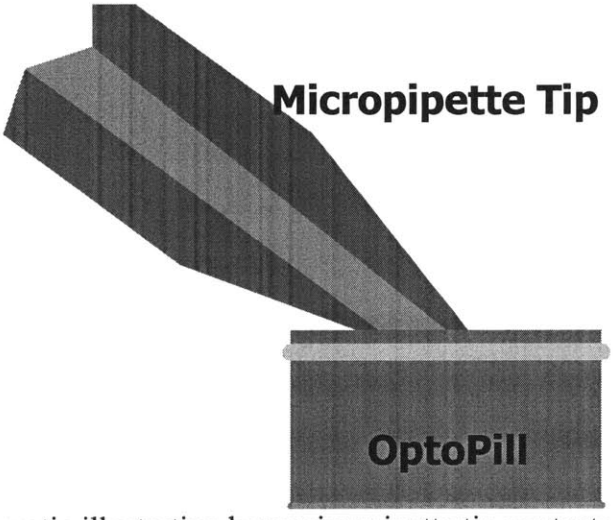

Figure 3-7 Schematic illustrating how micropipette tip contacts the top surface of an optopill.

The micropipette is positioned atop dispensed pills that are oriented right-side up, with the micropipette tip directly in contact with the pill surface. This is illustrated in Figure 3-7. The pill is picked up using vacuum pressure. A vacuum pump is hooked up to the micropipette holder to apply this vacuum pressure. The pill is placed onto the target recess (or substrate) either by merely releasing the vacuum pressure to atmospheric pressure or applying a slightly higher positive pressure using a neutral gas like argon.

3.2.1. Determination of Micropipette Tip Design

The first step to developing the vacuum tool MPAP technique was to find a suitably designed micropipette that could serve as an efficient pick-up tool. The initial choices for this purpose were glass micropipettes manufactured by Sutter Instruments. The tips of these micropipettes could be pulled into different shapes and sizes to suit their application. The micropipettes were pulled from 1mm outer diameter (O.D.) by 0.5 mm inner diameter (I.D.) glass tubing. Micropipettes with several variations in their design were experimented with to determine an optimum design for pill pick-and-place.

The first variation was the O.D. of the micropipette tips, from 25 μm to 45 μm. A larger diameter micropipette offered the advantage of a larger rate of flow of gas through the micropipette resulting in a more effective vacuum pressure and was thus preferred. However, it was necessary that the O.D. of the micropipette was smaller than the optopill surface so that the pills could be viewed clearly using a microscope while maneuvering the pipette atop the pill. As the diameter of pills used ranged between 35 to 50 μm, it was determined that a 35 μm O.D. micropipette tip was the optimum size.

Another variation was the shape and angle of the tip of the pipette. Two designs were tested, one with no taper in the tip and a 45 degree bevel, and the other with a 60 degree taper and a fire polished flat end with no bevel. Figure 3-8 provides a rough sketch of both designs. As the tips of the micropipettes had to be positioned in the micropipette holder such that the flat end of the tip was parallel to the flat substrate on which the pills were dispensed, it was much easier and faster to position the tapered

design. Conversely, the beveled design required much time for adjustment to ensure its edge was horizontal and parallel to the flat.

However, it was also found that the tapered design limited the field of view of the pills as much of the target pill would be blocked by the vertical end of the tapered tip. Moreover, the pipettes with the tapered edge had a longer, finer 10mm tip as opposed to the 8mm tips on the beveled pipettes, and were thus easier to break. Thus the beveled design was ultimately preferred. Nevertheless, the beveled glass micropipettes from Sutter Instruments were still relatively easy to break during handling and pill pick-up, and a harder material was desired.

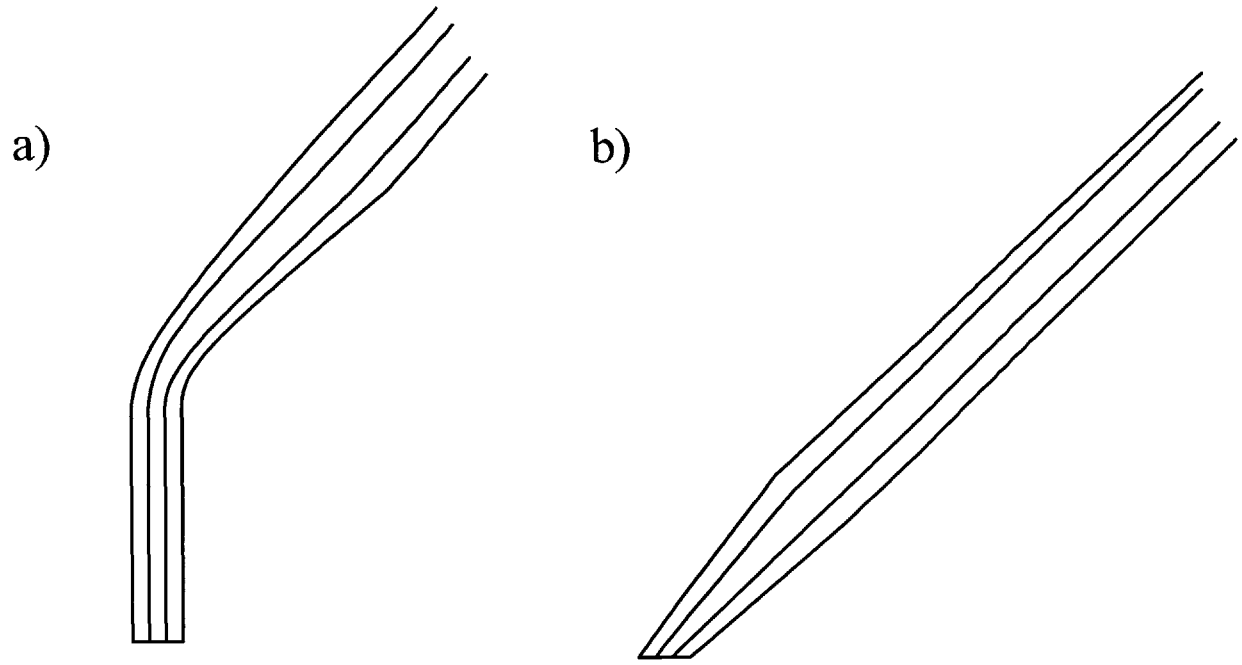

Figure 3-8 Micropipette tip designs that were tested (not to scale): a) Tapered micropipette tip. b) Beveled micropipette tip.

Quartz micropipettes with 35 μm O.D. tips beveled at 45 degrees from Precision Micro Devices were found to be better suited for MPAP due to their tougher material composition and shorter 6mm pulled tip [17]. These micropipettes were pulled from 1mm O.D. by 0.5 mm I.D. quartz tubing. These quartz micropipettes were used successfully to pick up optopills and place them both on flat substrates and in recesses. There was no pill breakage that occurred during pill pick-up, and the pills could be released from the

micropipette tips into their target locations by applying a positive pressure through the micropipettes using argon.

Thus, it was found that using clean quartz micropipettes with a 35 μm O.D. tip beveled at 45° and applying vacuum pressure through the micropipettes, optopills could be assembled onto their target recesses. The amount of vacuum pressure applied at the micropipette tip was measured to be approximately 0.1 atm or 1.5 psi. This vacuum tool MPAP provides a cleaner alternative to probe tip MPAP as no chemicals come in contact with the pills and pill breakage does not pose a problem.

It should be noted here that the micropipette tip design provides a degree of flexibility for various systems. The micropipette tip size may be changed according to the optopill size, and the tip design may be optimized to suit the specific set-up available for vacuum tool MPAP. For instance, if this MPAP technique is to be automated, a straight, non-tapered and non-beveled micropipette tip like that shown in Figure 3-9 may be desired.

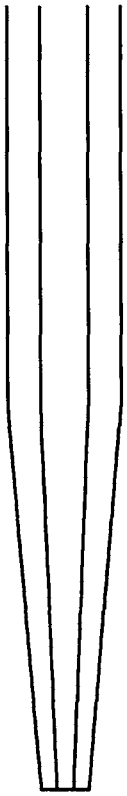

Figure 3-9 Schematic of a pulled micropipette tip that is not tapered or beveled (not to scale).

3.2.2. Micropipette Storage and Cleaning Procedures

The micropipettes from Precision Micro Devices were prone to attracting static dust and were water adsorbent. Therefore, care had to be taken during storage of the micropipettes. The micropipettes were kept in a static dissipative case to prevent accumulation of charged particles within the case. The case was stored in a desiccator cabinet when the micropipettes were not in use to minimize the hydration of the glass. When taken out of the cabinet, the case was kept in two layers of ziplock bags with a packet of desiccant between the two bags to adsorb moisture. The ziplock bag helped to keep dust off the case. The desiccant could not be placed directly in contact with the case as the desiccant packet shed.

Despite these measures, the micropipettes tended to attract dust particles and solvent residue (since the optopills had been dispensed in solvent), and adsorb moisture during use for MPAP. A methodical way of cleaning the micropipettes had to be designed in order to enable reuse of the micropipettes.

Personnel at Precision Micro Devices recommended using solvents like acetone or isopropanol to clean the micropipettes. Initial cleaning attempts involved using squirt bottles to project a narrow stream of acetone, methanol and isopropanol through the micropipette. The micropipette was then dried using a nitrogen air gun directed as best as possible down the middle of one end of the micropipette. The micropipettes cleaned this way were examined under a microscope. While the solvent had been successfully evaporated using the air gun, there was still a significant amount of particulates that had not been removed from the micropipette tip. Thus it was determined that the squirt bottle method was insufficient for removing debris from the micropipette tip.

A sonication cleaning method was tried instead. The micropipettes were held by a clamp and suspended in a beaker of acetone. This beaker was positioned in a 40 kHz ultrasonicator and sonicated for 10 minutes. Using squirt bottles, methanol and isopropanol were then squirted around and through the micropipettes. These micropipettes were then blown dry with an air gun in the manner described previously. It was found that this cleaning procedure was able to remove all particulates that were

visible under the microscope from the micropipettes. This sonication and blow dry method was adopted for cleaning the micropipettes for MPAP reuse.

These micropipette storage and cleaning procedures are summarized in Appendix A.

Chapter 4

Vacuum Film Bonding

4.1. Introduction to Optopill-to-Recess Bonding Issues

A technique for bonding the assembled optopills into their target recesses had to be devised. Good quality, robust bonds between the optopills and the recesses are necessary to ensure the optopills stayed in place for post-assembly processing. Ideally, the bond would also provide for a good ohmic contact between the underlying circuitry and the heterostructure device.

There were two main issues that had to be considered when designing this optopill-to-recess bonding technique. One of them was the need for a suitable metallurgical stack that fulfills both optopill-to-recess bond requirements stated above. Several bonding stacks were investigated. While most of these bonding stacks utilized the eutectic AuSn alloy as a soldering agent, a Pd/Sn/Pd stack was also investigated. The results of the study of these bonding stacks will be discussed in Chapter 5.

The other pressing concern was to find a suitable method of applying uniform static pressure on the optopills in recesses during bonding. This static pressure was necessary to promote effective bond formation and improve bond quality, especially for the metallurgical stacks that were being studied. This was evident based on the results presented in [18] – [24]. This chapter discusses the development of a vacuum film bonding system to address this issue.

4.2. Initial Pressure Application Methods

Two relatively crude methods of applying pressure during the bonding process were first attempted. The first utilized cover slips and weights to apply pressure on the optopills, as illustrated in Figure 4-1. A cover slip was first placed atop the sample to be bonded. A weight or several cover slips were then stacked atop this first cover slip to apply additional pressure during bonding.

Several papers [18]-[20] suggested bonding pressures of at least 10 psi. Each cover slip weighed 0.144 g and each optopill had an average diameter of 40 μm. Therefore, for each cover slip placed over 20 pills at one time, the pressure exerted would be approximately 8.4 psi. Thus two cover slips should be able to exert the minimum required amount of pressure for bonding.

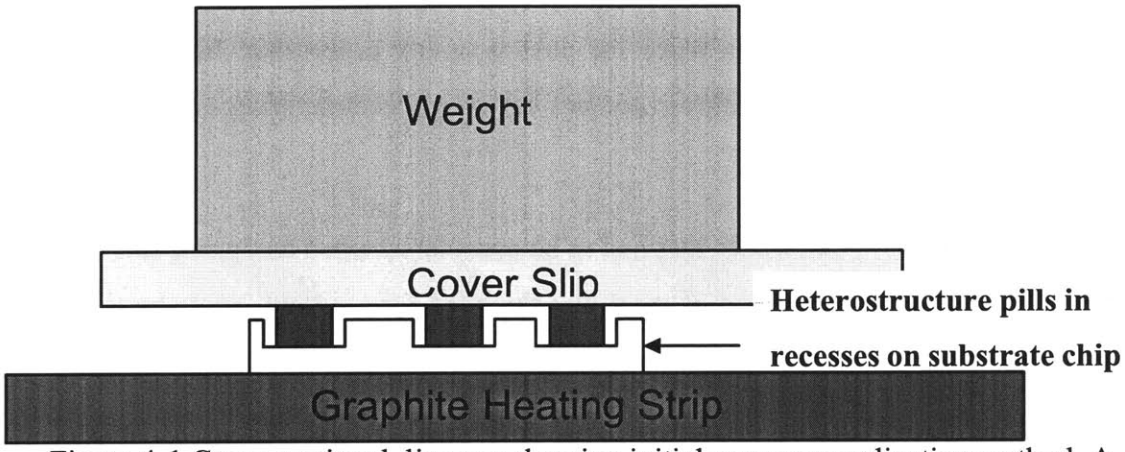

Figure 4-1 Cross-sectional diagram showing initial pressure application method. A weight was placed atop a glass slide that was in turn placed atop the sample to be bonded. The weight was sometime replaced with several glass slides stacked atop the first glass slide.

Indeed, it was found possible to get some pills to bond this way using 0.6 μm of AuSn on the bottom of the pills and a Cr/Au/Cu/Au (0.05/0.02/0.5/.02 μm) metallization for the recess pads. However, the yield was very low (<50 %). It was determined that the success of this method was very dependent on all the pills and recesses being of uniform height and depth respectively. Moreover, the surfaces of the pills and the recesses had to be completely flat in order for the glass slide to exert uniform pressure on each pill. This

method of applying pressure also limited the depth of the recess with respect to the optopill height, as the optopills had to be thick enough to stick out of the recess.

Due to process limitations, it would be very difficult to ensure that all the pills were of uniform height and all the recesses were of uniform depth and all the surfaces involved were completely flat. This was thus an impractical method of pressure application.

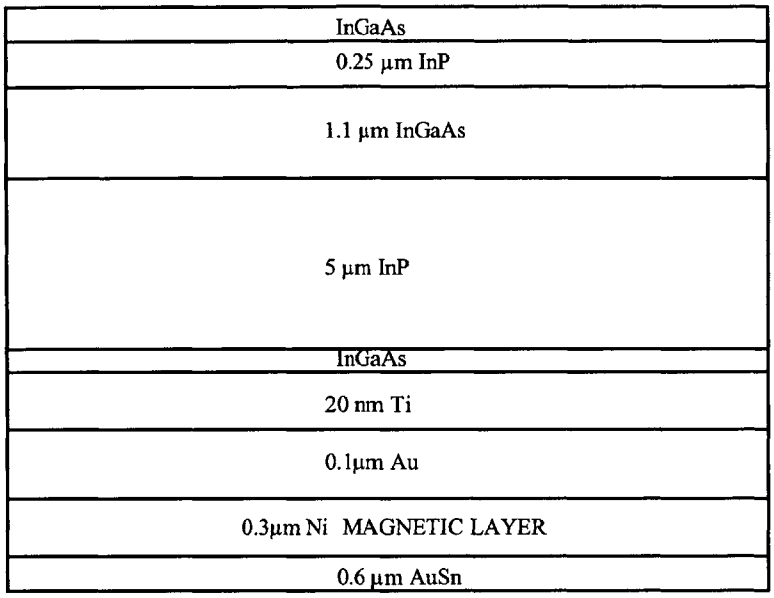

Figure 4-2 Schematic of optopill used for bonding using magnetic attraction to hold the pill down (not to scale). These optopills were bonded to recesses that had Cr/Au/Cu/Au (0.05/0.02/0.5/.02 μm) pads deposited in them. Note the magnetic layer of Ni deposited before the AuSn layer.

A second pressure application technique was attempted. This involved using magnetic forces to hold the pills down in the recesses during bonding. A layer of Ni, a magnetic material, was deposited on the pills so that they would be attracted to the magnet placed below the graphite heating strip. A samarium cobalt permanent disc magnet was chosen to provide a strong magnetic field. The size was chosen to be 0.75" diameter to ensure that the entire area of the 1 cm^2 substrates that the optopills were placed on would be directly above the magnet. The structure of the optopills used and the bonding system set-up for this magnetic attraction method is illustrated in Figures 4-2 and 4-3 respectively. The magnet was placed as close to the heating strip as possible.

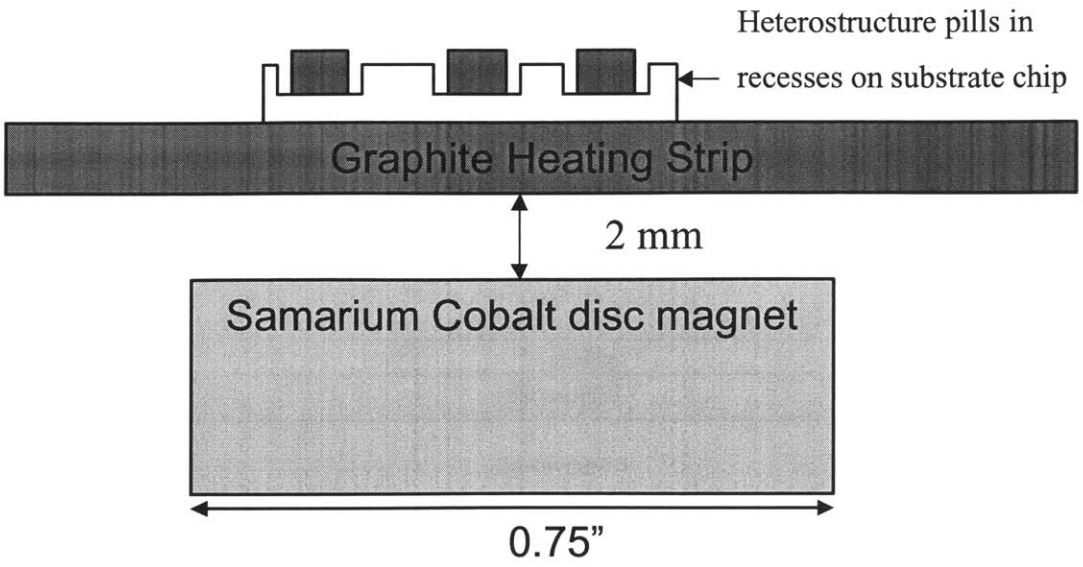

Figure 4-3 Cross-sectional diagram showing set-up for bonding using magnetic attractive forces to hold pills down in recesses (not to scale). Note that the substrate chip is smaller than the disc magnet.

Although it was possible to bond some pills to recesses using this magnetic attraction force, it was difficult to quantize the magnetic forces involved and evaluate the exact force exerted on the pills during bonding. It was hard to tell if a uniform force was exerted on each pill during bonding. This method of pressure application also implied that all the optopills bonded this way would have to include a layer of magnetic material in their metal stack, imposing limitations on the optopill structure.

A more sophisticated method of pressure application during bonding was therefore required. A technique that could ensure uniform pressure application on all pills, independent of relative pill height and recess depth, without limiting the optopill structure design, was desired.

4.3. Vacuum Film Bonding Technique

A vacuum-bagging bonding apparatus used to bond 5 mm x 5 mm GaAs chips to similarly sized Si chips under pressures of 14 to 55 psi had been described by G. R. Dohle, et al [18], [19]. The use of this vacuum bagging technique ensured uniform pressure on the bonding samples, independent of variations in the sample thickness and

smoothness. It was therefore thought that a bonding system based on the same principles could be designed for bonding the optopills to recesses.

4.3.1. Vacuum Film Selection

In order to develop such a bonding set-up, a suitable vacuum film had to be found first. This film would have to be sufficiently flexible to conform to the shape of the pills and able to tolerate the bonding temperatures used. Typical bonding temperatures that were used for optopill bonding lay in the range from 280 to 370 °C. The film had to be able to withstand the bonding pressures of up to 50 psi. It was also preferable that the film be transparent or translucent to allow for a view of the sample during bonding. This would enable the user to determine if the sample was displaced during chamber evacuation or in-gassing prior to or after bonding.

Material Properties	Values
Tensile Strength	>24000 psi
Maximum use temperature	400 °C
Elongation at break	45 %
Color	Light amber, transparent
Density	1.42 g cm^{-3}
Shelf life	18 months

Table 4-1 Thermalimide Material Properties

Thermalimide, an ultra high temperature bagging film typically used for vacuum bagging applications like those in the aerospace and automotive industries, was found to suit the above vacuum film requirements. Thermalimide is an inert polyimide film. Its properties are summarized in Table 4-1. This bagging film was supplied by Airtech Advanced Materials Group [25]. Figure 4-4 provides an image of this yellow transparent film as it was used in the bonding set-up.

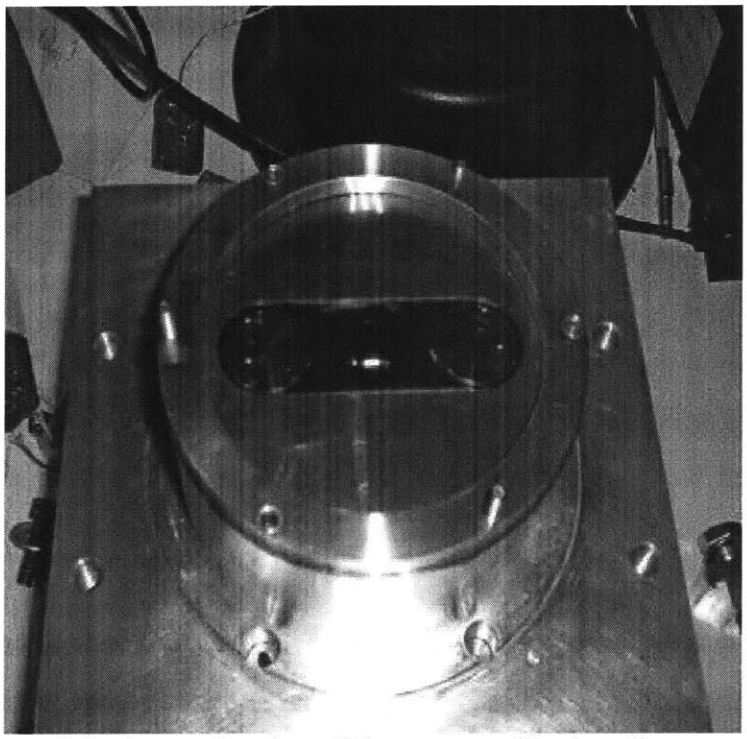

Figure 4-4 Image of the inner chamber of the vacuum film bonding system. The amber film shown is Thermalimide. The graphite heating strip is visible from the oblong gap in the metal frame supporting the vacuum film.

4.3.2. Vacuum Film Bonding Apparatus Design

Using Thermalimide as the vacuum film, a vacuum film bonding apparatus was designed according to the schematics shown in Figure 4-5. These schematics were drawn by Prof C. G. Fonstad, Jr. This bonding apparatus consisted of an inner chamber and outer chamber. A 0.040" thick graphite strip was used as the heating strip and positioned in the inner chamber. This graphite strip could withstand up to 38 psi of pressure before breaking. A K-type thermocouple was attached to the center of the graphite strip using high temperature resistant cement. The sample to be bonded was to be placed on the graphite strip.

The vacuum film was supported by a metal frame and placed directly above the graphite strip. This metal frame and the vacuum film served as a barrier separating the inner chamber from the outer chamber. An oblong hole in the metal frame was positioned such that the entire graphite strip and the sample placed on it would be visible and in direct contact with the vacuum film during pressure application, when the vacuum film

would deform to the contours of the sample. The vacuum film was replaced every 3 or 4 bonding runs to ensure a relatively clean film surface came into contact with the bonding samples each time.

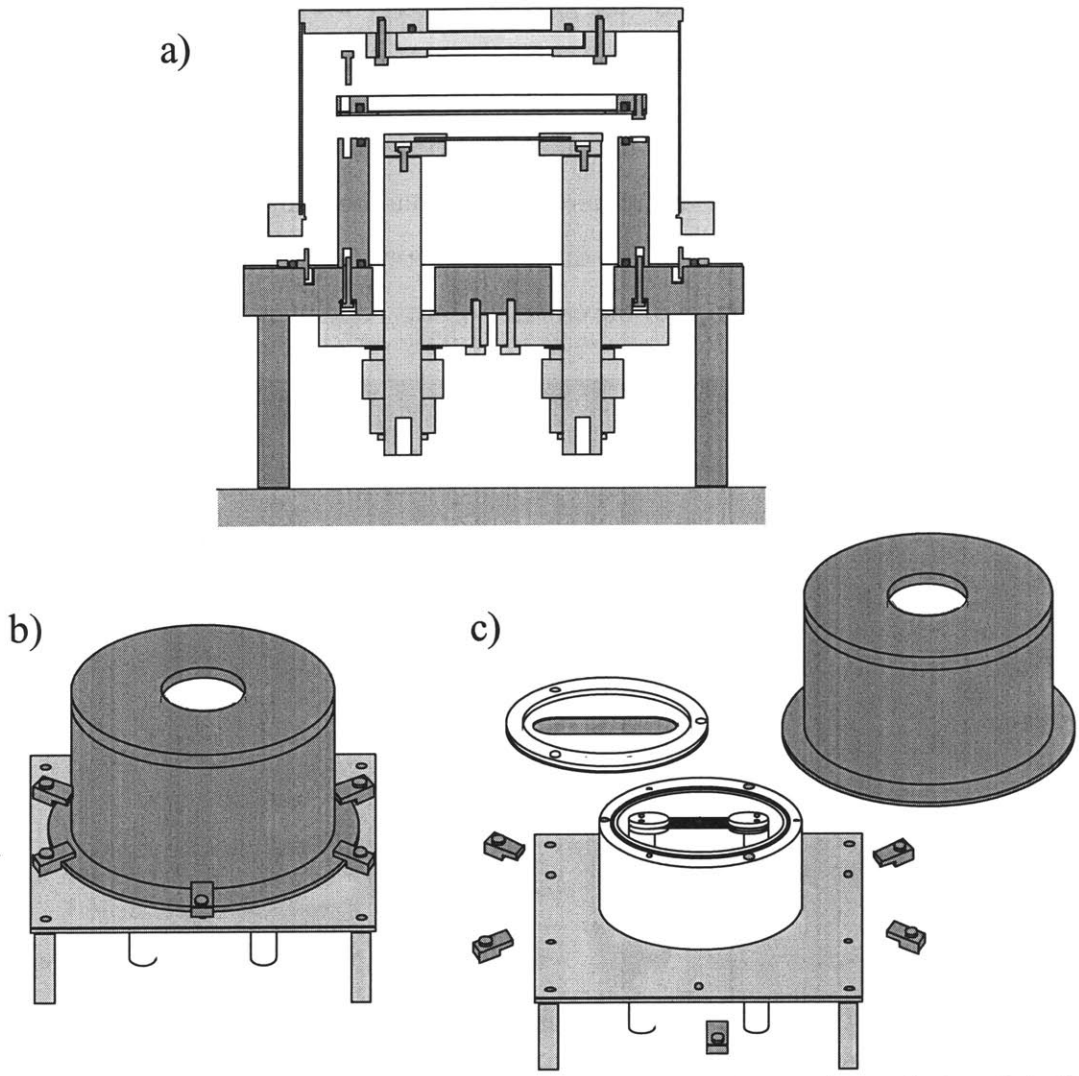

Figure 4-5 Schematics of vacuum film bonding apparatus design drawn by Prof C. G. Fonstad, Jr. a) Cross-sectional view of inner and outer chambers. b) Exterior view of bonding apparatus. c) Alternate view of inner and outer chambers.

Due to concerns that there might be a need for a higher bonding pressure than 38 psi, a 0.04" thick ceramic strip was used to reinforce the graphite heating strip when necessary. This ceramic strip had a hole drilled in it for the thermocouple attached to the heating strip to pass through. The combination of the ceramic strip and graphite strip could easily tolerate more than 50 psi of pressure.

After the samples to be bonded were placed on the heating strip, and the vacuum film was clamped in place, forming gas (95 % nitrogen, 5 % hydrogen) was flowed through and out of the inner chamber for 10 min to flush out any atmospheric air in the inner chamber. The outflow valve from the inner chamber was closed during bonding, while maintaining a flow of forming gas, to regulate the inner chamber pressure at approximately 1 psi. This reducing gas mixture was used to minimize oxidation.

Nitrogen was flowed through the outer chamber and the nitrogen flow was adjusted according to the bonding pressure required. The actual bonding pressure exerted on the sample in the inner chamber was the difference between the outer and inner chamber pressures. Figure 4-6 is an image of the exterior of this bonding apparatus.

Figure 4-6 Image of exterior of actual bonding apparatus.

The temperature of the heating strip was adjusted using a Eurotherm controller that was connected to the thermocouple. The controller had both a manual and an automatic mode. The manual mode enabled live adjustment of the power fed to the bonding system and thus variation of the temperature. The automatic mode allowed the user to program temperature ramp rates, target temperatures and temperature hold durations for a single bonding run. The latter mode was used for all bonding runs. Ramp rates of up to 100

°C/min were programmed and run successfully, i.e. the thermocouple readings corresponded to the programmed temperature sequence.

This apparatus could also be converted to a regular annealer by removing the vacuum film and its supporting frame. Once this divider between the inner and outer chambers was removed, the entire chamber could be flushed with forming gas and used for annealing purposes.

As will be discussed in the next chapter, it was found that this vacuum film bonding apparatus was a suitable solution to applying uniform static pressure on the samples during bonding.

Chapter 5

Bonding Experiments

5.1. Overview of Bonding Experiments

Several metal stacks were tested to find a suitable bonding scheme to bond the optopills to their target recesses. The ideal bonding stack has to satisfy two main criteria. Firstly, it has to ensure a strong, robust bond between each optopill and its target recess. Secondly, it should also provide for good ohmic contact between the optopill and the underlying circuitry of the target substrate. In addition, it is preferable that the bonding temperature is kept within a reasonable range that will not significantly degrade the performance of the underlying circuitry.

The bonding capabilities of the metal stacks were tested using three types of bonding experiments. The first involved bonding 2 flat Si substrates that had been coated with the desired metal stacks. Such an experiment was useful for observing the behavior of the metal stacks at bonding temperatures due to the larger surface areas involved. The second entailed bonding optopills to flat Si substrates. Metal stacks were deposited on the polished Si substrates using an electron beam (e-beam) evaporator, while the metal stacks for the optopills were sputtered on during pill processing. This was mostly performed by J.J. Rumpler and J. M. Perkins. This type of experiment was useful as it was easier to push at the optopills and thus test the strength of the bond when they were bonded flat substrates instead of in recesses. The third type of experiment involved bonding optopills to pads in dummy recesses. The optopills used were 35 - 45 μm in diameter.

These dummy recesses simulated actual device recesses on IC chips, and were processed on highly doped (> 10^{19} B) p-type Si pieces. The low resistivity of this Si substrate (0.0010 – 0.0020 Ω cm) ensured the ease of testing electrical connectivity between the pills and the underlying substrate. Silicon oxide was deposited on the Si chips and patterned into arrays of 50 μm – 60 μm square recesses that were approximately 5 – 5.3 μm deep.

This was preferable to etching the recesses directly in silicon, because by etching the recesses in oxide, the polished silicon surface acted as an etch stop layer. This ensured that the base of the recesses was smooth. This was crucial as any surface roughness would translate to a rough bonding surface, since the metal stacks were deposited directly on the base of the recesses. This would prevent the formation of good quality bonds between the optopills and recesses. The cross-sectional profile of a typical dummy recess is shown in Figure 5-1. The metal stacks were deposited and patterned in these recesses using the electron beam evaporator and lift-off lithography. Processing recipes used for these procedures are listed in detail in Appendix B.

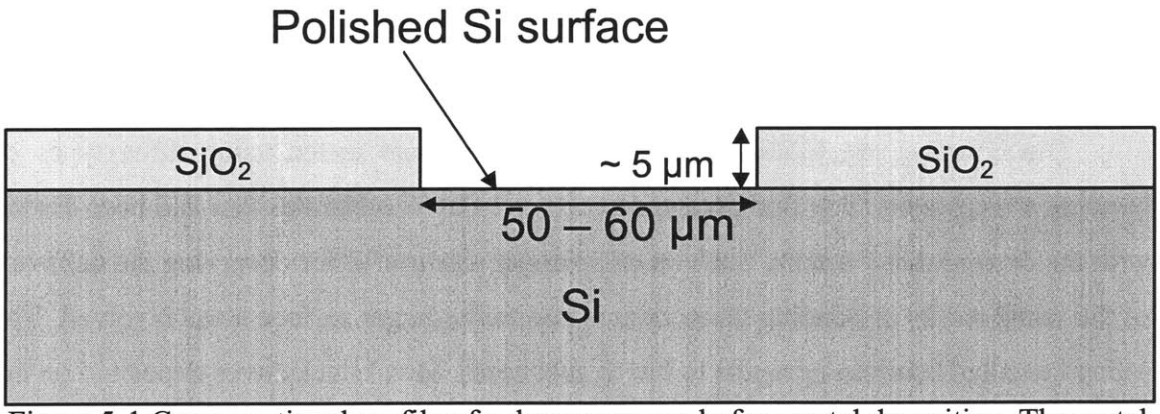

Figure 5-1 Cross-sectional profile of a dummy recess before metal deposition. The metal stack is deposited atop the polished Si surface (i.e. the recess base).

5.2. AuSn to Cr/Au/Cu and AuSn to Cr/Au/Cu/Au

AuSn (20 wt % Sn) eutectic performs have been used in several bonding applications such as flip chip bonding. It is preferred for its relatively low melting point of 282 °C [26], excellent electrical and thermal conductivity, high mechanical strength, superior high temperature performance and fluxless soldering. The low melting

temperature implies a low bonding temperature and thus ensures minimal thermally induced damage to the optopills and the underlying circuitry. The phase diagram for the Au-Sn system is provided in Figure 5-2. Several bonding schemes using AuSn were investigated for optopill to recess bonding.

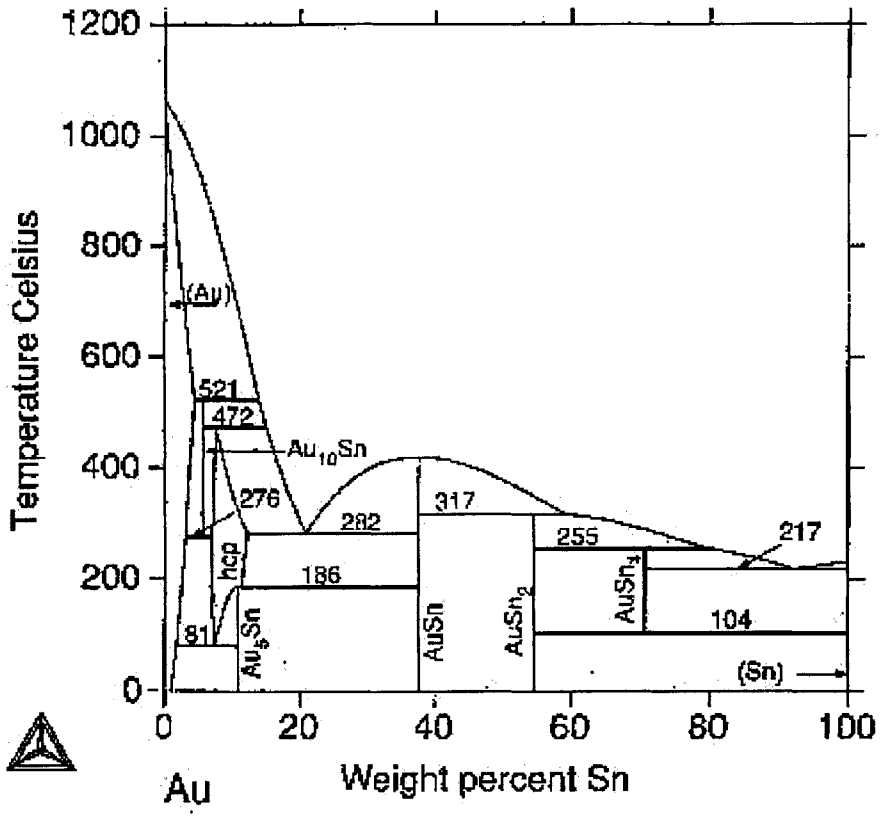

Figure 5-2 Phase diagram for Au-Sn system. Taken from http://web.met.kth.se/dct/pd/element/Au-Sn.html.

The first bonding scheme tested involved bonding AuSn coated optopills to a Cr/Au/Cu stack, with Cu serving as the wetting surface for the AuSn solder. One type of bonding test was carried out for this metallurgical scheme. This was optopill-to-flat-Si substrate bonding. 0.6 μm of the preform AuSn eutectic was deposited on the optopills. The optopills used were p-i-n diodes of the structure shown in Figure 5-3 and were processed by E. Atmaca. Cr/Au/Cu (0.05/0.02/0.5 μm) stacks were deposited via an e-beam evaporator onto the flat Si substrates. All three metals in the stack were deposited in a single vacuum cycle to prevent problems of oxidation of the intermediate layers due to exposure to atmospheric air between the deposition of each layer.

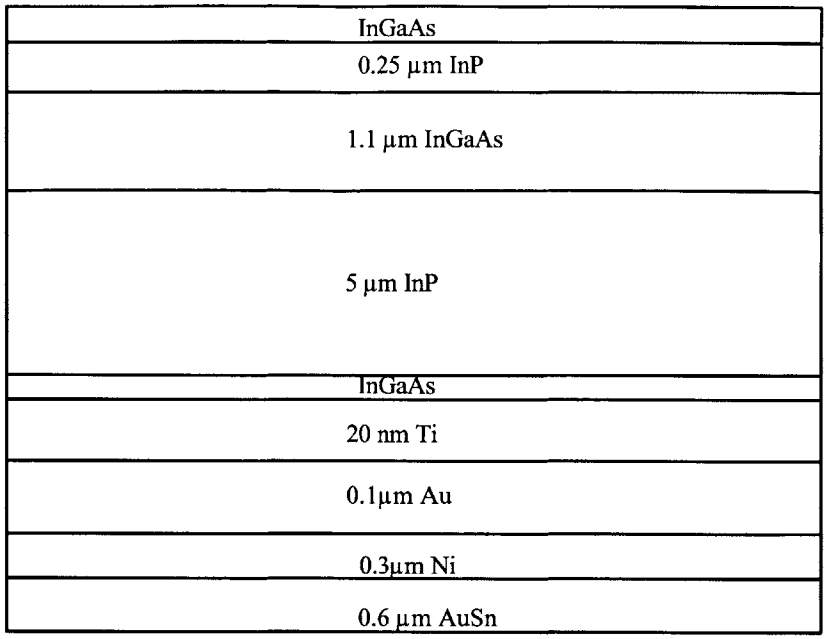

Figure 5-3 Structure of p-i-n diode heterostructures with AuSn layer.

The top Cu layer was to serve as the wetting surface for the AuSn on the optopill to melt and bond to. Initially, a Ta/Cu stack was tried, with the Ta layer acting as an adhesive layer between Si and Cu. However, the high temperatures involved in Ta deposition using the e-beam tended to burn the thick photoresist (AZ 4620) on dummy recess substrates. This made it impossible for lift-off. An alternative adhesive layer had to be used. Cr has been established as a good adhesion layer between Si and Au, and there is no problem of adhesion between Au and Cu. Thus, a thin Cr/Au layer (0.05/0.02 μm) was deposited on the Si before the 0.5 μm Cu layer.

At the time of these experiments, both vacuum tool MPAP and the vacuum film bonding technique had not been developed yet, so their precursors were used to place and bond pills with this metallization scheme. Optopills were placed atop flat substrates with this Cr/Au/Cu metallization using solder flux probe tip MPAP. They were bonded down using the magnetic attractive forces technique described in Chapter 4, whereby a permanent magnet was placed directly under the heating strip where the sample was placed. The 0.3 μm layer of ferromagnetic Ni in these optopills enabled them to be attracted to the permanent magnet and therefore held down onto the flat Si substrate during bonding.

Bonding temperatures were varied between 300 °C to 400 °C and bonding times were varied from 2 minutes to 10 minutes. Bonding time refer to the duration that the temperature of the heating strip was held at the bonding temperature. The bonding temperature was ramped up from room temperature at a rate of 50 °C/min and ramped down at the same rate. Each bonded sample was solvent cleaned with acetone, methanol and isopropanol and blown dry with a nitrogen gun. This was done to attempt to remove any pills that had not bonded at all.

Bonding strength was tested in 2 consecutive ways. The first was a top-lift test that attempted to lift the bonded pill using probe tip MPAP. If the pill stayed in place, a second test was administered. This was a push test that involved pushing repeatedly (at least 3 times or until the pill budged or broke) on the side of the pill using a probe tip. If the pill was not removed by this second push test, or broke during the push test, it was deemed to have a reasonably strong bond to the flat substrate, as this indicated that the bond strength was stronger than the heterostructure itself. The results of the bonding tests are summarized in Table 5-1.

Initially the Cu surfaces were only cleaned with solvents (acetone, methanol and isopropanol) and blown dry before pill placement and bonding. It was found that none of the pills that were bonded on these surfaces stayed in place after the probe tip push test. These pills did not leave any residue either, indicating that there was no significant wetting of the Cu surface with the AuSn solder from the pills. It was concluded that the poor bonding results were due to oxidation of the Cu surface, as oxide is a very poor wetting surface. Its presence would affect the quality of the bond formed between the pill and the Cu surface, if any was formed at all.

An HCL clean of the flat Si substrate was thus implemented right before pills were placed and bonded on the Cu coated surface of the substrate. This HCL clean involved a one minute dip in a 1:1 HCL:DI H_2O solution, followed by a dip in DI water in few seconds, and a nitrogen gun blow dry. The removal of the oxide from the Cu surface also made it much easier to place pills by probe tip MPAP, as there was a noticeable attractive

force between the pills and the Cu once they were in contact. A second probe tip was not required to aid in nudging the pills off the first probe tip during pill placement.

Sample No.	Initial no. of pills placed	Bonding Temp. (°C)	Bonding Time (min)	No. of pills left in place		No. of pills broken during or left in place after push test (i.e. good bond)	No. of pills that left a residue after being removed completely (not including broken pills)
				after solvent clean	after top-lift test		
1 (no HCL clean)	10	300	2	8	5	0	0
2 (no HCL clean)	6	380	4	6	6	0	0
3	10	300	2	10	10	0	2
4	7	380	4	7	6	2	4
5	8	340	4	8	8	3	2
6	5	340	4	5	5	5	N.A.

Table 5-1 Summary of results of bonding AuSn coated optopills to Cr/Au/Cu (0.05/0.02/0.5 μm) coated flat Si substrates. Apart from the first 2 samples listed in the table, all Si substrates used in these experiments were cleaned in a HCL dip, to remove any Cu oxides due to exposure of the top Cu surface to atmosphere, immediately before pill placement. The pills were held down during bonding using the magnetic attractive force technique. Bonding temperature was ramped up and down at a 50 °C/min rate.

Although the melting point of the AuSn eutectic is 282 °C, it was found that the pills bonded at 300 °C on HCL cleaned Cu surfaces did not adhere well to the flat substrates. Increasing the bonding temperature to 380 °C did improve the results, as 2 out of 7 pills broke during or remained in place after the push test, and 4 pills left a residue after being pushed off, indicating that the AuSn solder from these 4 pills did wet the Cu surface. The residue was partly attributed to possible poor adhesion between the semiconductor material of the pills and the metal layers deposited on the pills.

The bonding temperature was then reduced to 340 °C. Bonding at this lowered temperature did not adversely affect the bonding results, and yielded reasonably good

results. For the two bonding runs done at this temperature, more than 75 % of the total number of pills placed and bonded passed the push test, either staying in place or breaking when pushed with a probe tip. Figure 5-4 is an SEM image of an AuSn coated pill that was successfully bonded to a HCL cleaned Cr/Au/Cu coated flat Si substrate during one of these bonding experiments.

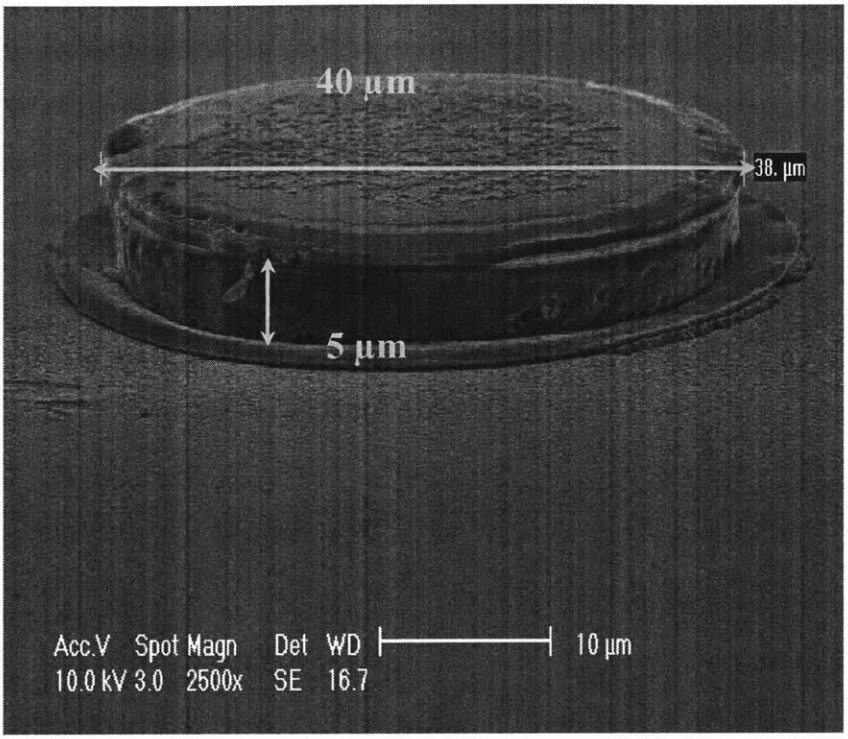

Figure 5-4 SEM image of AuSn coated optopill bonded to HCL cleaned Cr/Au/Cu coated flat Si substrate. The wider ring of metal around the base of the pill is the melted and reformed AuSn layer that had been deposited on the pill.

The lower bonding temperature of 340 °C was preferred over 380 °C as there was no significant difference between the results of bonding at the two temperatures. Thus, it was determined that for the Cr/Au/Cu to AuSn bonding scheme, bonding at 340 °C for 4 min was desirable. The discrepancy between the indicated bonding temperature and the melting point of the AuSn solder could be due to the fact that the bonding temperature is measured at the heating strip, and may not be the exact temperature of the bonding sample. Heat conduction between the strip and the sample had to be accounted for.

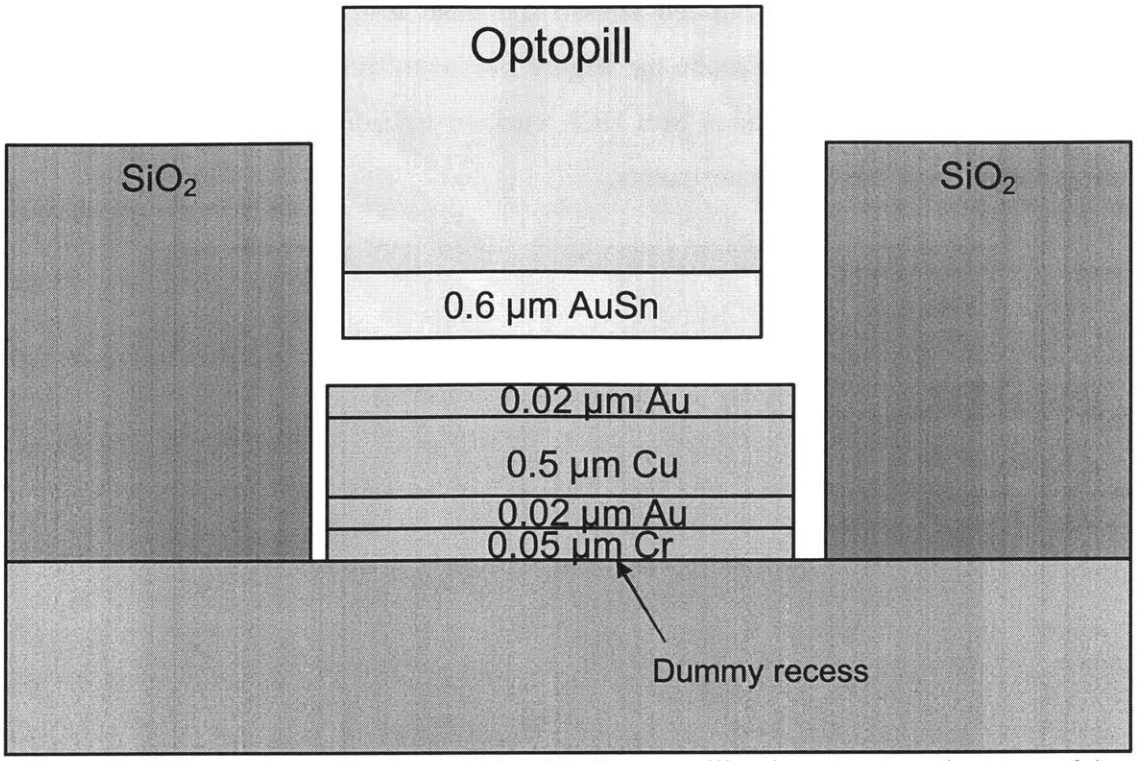

Figure 5-5 Illustration of AuSn to Cr/Au/Cu/Au metallization structure (not to scale).

In order to eliminate the necessity of a HCL clean of the Cu surface, a Cr/Au/Cu/Au (0.05/0.02/0.5/0.02 µm) stack was suggested, instead of the Cr/Au/Cu stack, for bonding to AuSn pills. This metallization scheme is illustrated in Figure 5-5. The thin, 20 nm top Au layer served to prevent oxidation of the underlying Cu layer. This metal stack was deposited in the dummy recesses described in the previous subsection. The recesses were solvent cleaned (acetone, methanol, isopropanol) and blown dry before optopill placement. The same AuSn optopills as those used for the Cr/Au/Cu bonding experiments (refer to Figure 5-2) were placed in these recesses and bonding was attempted. Due to the partial success of bonding AuSn pills to Cr/Au/Cu coated flat Si substrates at 340 °C for 4 min, similar bonding temperatures and times were used. Probe tip MPAP and the magnetic attractive force bonding technique was used again as vacuum tool MPAP and the vacuum film bonding apparatus had not been developed at the time of these experiments. The results of these bonding experiments are summarized in Table 5-2.

Sample No.	Initial no. of pills placed in recesses	Bonding Temp. (°C)	Bonding Time (min)	No. of pills left in place after solvent clean	No. of pills broken or left in place after top-lift and push tests (i.e. good bond)	Additional Notes
1	7	340	4	6	4	None of the 4 pills that remained in place after the top-lift and push tests were removed when a strong permanent magnet was placed atop the bonded sample
2	10	340	4	10	8	-
3	8	340	4	6	-	Attempts were made to pattern Ti/Au (0.02/0.2 μm) ohmic contact rings on the bonded pills using processes described in Appendix B. However, all the pills fell out during lift-off in acetone.
4	14	340	4	14	14	All 14 pills stayed in and Ti/Au (0.02/0.2 μm) ohmic contact rings were successfully patterned on the pills, even after immersing the sample in a beaker of acetone and ultrasonicating for 10 s.
5	10	340	4	10	10	All 10 pills stayed in and Ti/Au (0.02/0.2 μm) ohmic contact rings were successfully patterned on the pills

Table 5-2 Summary of results of bonding AuSn coated optopills to Cr/Au/Cu/Au (0.05/0.02/0.5/0.02 μm) pads deposited in dummy recesses. The pills were held down onto the bonding pads in the recesses during bonding using the magnetic attractive force technique. Bonding temperature was ramped up and down at a 50 °C/min rate.

Some of these samples underwent further tests after the probe tip top-lift and push tests. These tests are described in the Additional Notes column in Table 5-2. It was determined that quality bonds between optopills and recesses could be obtained using the Cr/Au/Cu/Au to AuSn bonding scheme. The first sample listed in Table 5-2 only had a 57 % yield, but the pills that stayed in after the probe tip top-lift and push test could not be removed by placing a strong magnet atop the bonding sample, even though they contained a magnetic Ni layer. The second sample had an 80 % yield. Three further samples were bonded and processed further to deposit and pattern ohmic contact rings (0.02/0.2 μm Ti/Au) on the bonded samples. While no pills were lost from two of these bonded samples during this post-assembly processing, all the pills on another bonded sample fell off during lift-off. Figure 5-6 is an SEM image of a bonded pill with a successfully patterned ohmic contact ring.

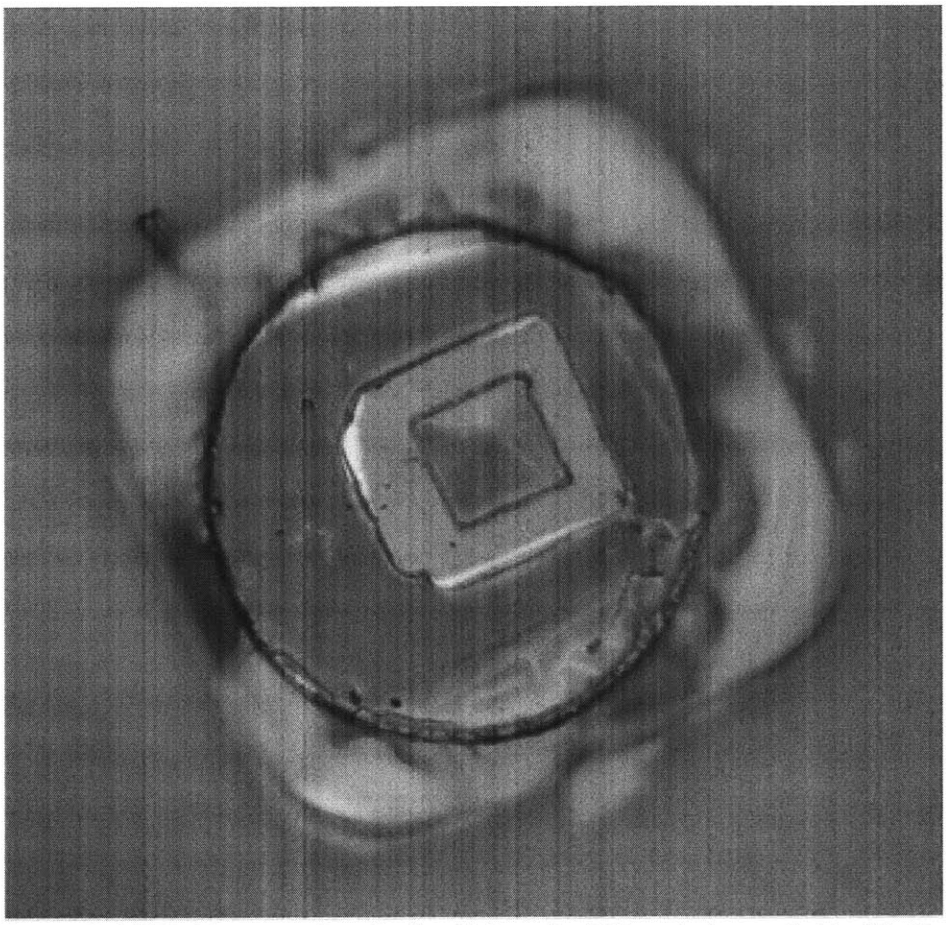

Figure 5-6 SEM image of an AuSn (0.6 μm) pill bonded to a Cr/Au/Cu/Au (0.05/0.02/0.5/0.02 μm) stack. A Ti/Au (0.02/0.2 μm) ohmic ring was successfully patterned on the top of the pill.

There could be several factors that contribute to the failure of these bonds. Oxidation of the AuSn solder on the optopill could affect the bonding dynamics. Moreover, the magnetic attractive force bonding technique may not have ensured that uniform and equal pressure was applied during bonding of each of the samples. The results indicate that while the 0.6 μm AuSn optopill to 0.05/0.02/0.5/0.02 μm Cr/Au/Cu/Au recess bonding scheme produced a high (sometimes even 100 %) yield per sample for some of the bonded samples, there is no 100 % guarantee that all the samples bonded using this scheme had sufficiently robust bonds to withstand post-assembly processing.

Indeed, despite its partial success with regards to bonding, the AuSn optopill to Cr/Au/Cu/Au recess metallization scheme left much to be desired. Firstly, having the AuSn on the optopill meant it was difficult to remove any oxidation of the AuSn by an acid clean due to the small size of the optopills. It would be more practical to have the AuSn solder deposited on the bottom of the recesses, as cleaning an entire chip with an array of recesses by an acid clean would be easier than cleaning the individual optopills. In addition, the Cr/Au/Cu/Au metallization did not provide a suitable ohmic contact to Si, thus failing to satisfy the electrical connectivity criteria of an ideal bond between an optopill and its target recess.

5.3. Cr/Au to Cr/Au/Sn/Au

Several papers [18]-[20] suggested using a suitably proportioned Sn/Au multilayer structure instead of the preform AuSn solder to address the issue of AuSn oxidation. This multilayer is deposited in one vacuum cycle to protect the Sn layer from oxidation. The outer Au layer protects the Sn layer from exposure to air. The Au/Sn multilayer can provide a similar bonding function as the AuSn preform because the melting point of Sn is lower than the eutectic point of the AuSn alloy [20].

5 mm x 5 mm GaAs dummy chips or "coupons" had been successfully bonded to 5 mm x 5 mm Si dummy coupons using a Cr/Au (0.07/1.6 μm) to Cr/Au/Sn/Au (0.07/0.175/0.815/0.0475 μm) multilayer structure. If the Au and Sn layers of both of these bonding structures formed a uniform Au-Sn alloy, the alloy would have 84 wt %

Au, close to the eutectic AuSn composition (80 wt % Au). This was accomplished by G.R. Dohle, et al., by bonding at temperatures of 286 °C for 30s and applying static pressures of 14.7 psi (1 atm) [18]. On the other hand, C. C. Lee, et al., suggested that the temperature would have to raised above 309 °C the Au/Sn composite to become an alloy solution and dissolve the gold layers to form a near-eutectic AuSn alloy [20]. Bonding pressures of 40 psi and bonding times of 13 min were cited in this second paper.

However, the total metal thickness of at least 2.5 μm that was used for bonding in both examples cited above was too thick for optopill-to-recess bonding, since the optopill itself was only about 5 μm in thickness. Such a thick bonding layer may melt and form over the sides of the optopill during bonding under pressure and is undesirable. For instance, this may interrupt the interface between an optopill designed for laser applications and a planar waveguide on its target substrate. Therefore, bonding experiments had to be conducted to determine if a thinner Au/Sn multilayer structure than those cited above could be used successfully for bonding.

Attempts were first made to recreate the results of bonding larger test coupons (5 mm x 5 mm each) using a significantly thinner Au/Sn multilayer structure than those used in [18]-[20]. Cr/Au (0.07/0.8 μm) was e-beamed onto the polished surface of a Si wafer. The Cr/Au/Sn/Au composite structure was deposited on the polished surface of another Si wafer. The thicknesses of the metal layers in this composite were 0.07, 0.01, 0.415 and 0.024 μm respectively. The total metal thickness was approximate half of that suggested in [18]. Each wafer was cleaved into pieces that were approximately 5 mm x 5 mm in size for bonding. This metallization scheme is illustrated in Figure 5-7a. The relative thicknesses of the Au and Sn layers were maintained to ensure a near eutectic proportion with 84 wt % Au.

The test coupons were solvent cleaned (acetone, methanol, isopropanol) and blown dry immediately before bonding. As the vacuum film bonding system was developed only midway through this study, static pressure was applied to the initial samples using 2 metal weights atop 2 glass cover slips to distribute the pressure. Using this set-up, three samples were bonded at 380 °C for 10 min, and one sample was bonded at 350 °C for 30

min. The temperature was ramped up and down at 40 °C/min for all four samples. While the bonded pieces could not be pushed apart using tweezers to push on one edge of the bonded samples, they could be pulled apart, without the semiconductor pieces breaking, using two pairs of tweezers. The bonds formed between the bonded pieces were thus deemed to be insufficiently robust for the optopill to recess bonding application.

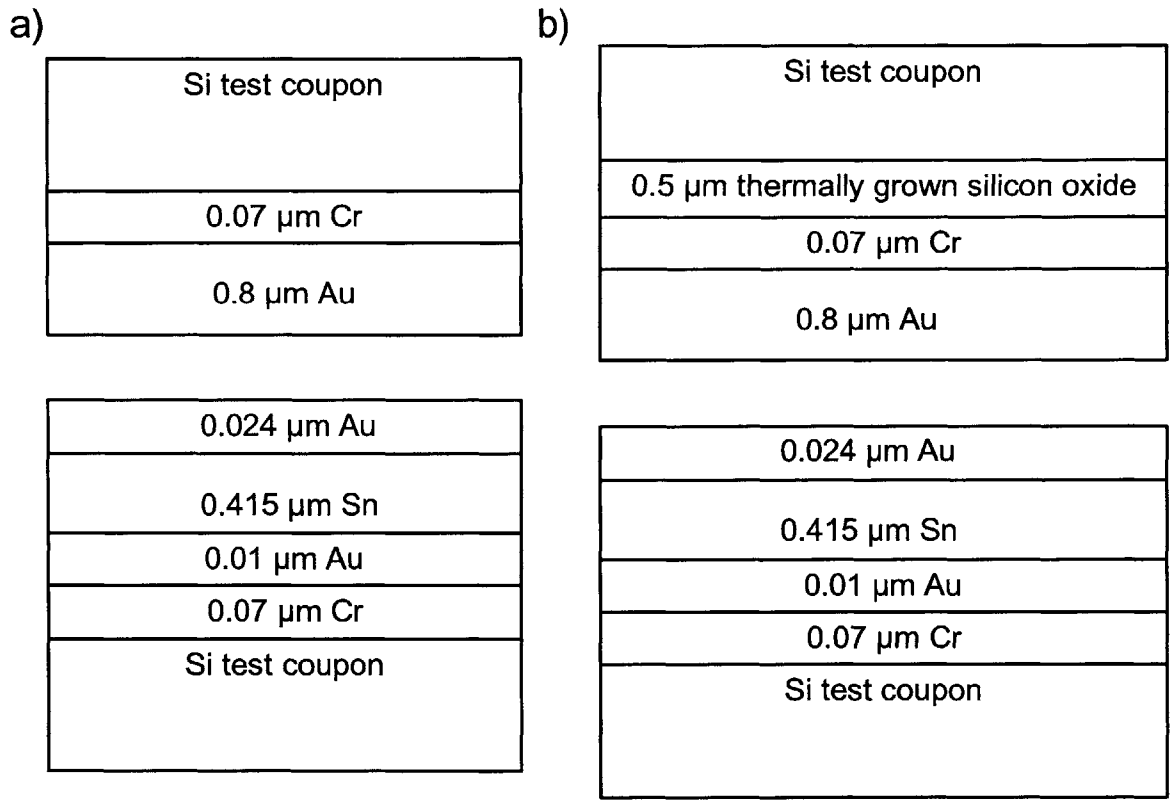

Figure 5-7 Illustration of Cr/Au to Cr/Au/Sn/Au metallization structure (not to scale). a) No oxide barrier to prevent Au diffusion into Si. b) An oxide barrier was thermally grown before deposition of the Cr/Au layer to prevent diffusion of Au into Si.

Observing the post-bonding surface of the pairs of coupons after they had been pulled apart, it was obvious that only patches of the metal stacks on both sides of the bonding scheme had reacted, as there was little change in some areas compared to the pre-bonding appearance of the metal stacks. This was possibly due to the insufficient and non-uniform static pressure applied on the samples by the weights. The vacuum film bonding set-up was developed in part to overcome this problem. In addition, spiral-like structures were observed on the Cr/Au surface under the microscope. These structures

were indicative that the Au was diffusing in to the Si. This was highly possible due to the very low diffusion 0.4 eV activation energy of Au into Si.

This would affect the bonding mechanism, so 5000 Å of oxide was thermally grown on the polished surface of a Si wafer to serve as a diffusion barrier. The Cr/Au metal stack was deposited on the oxide surface instead of directly on the Si surface. This is illustrated in Figure 5-7b. This metallization scheme was used for the next bonding experiment described here. The vacuum film bonding system was developed in time for this experiment.

Two Si test coupons with the thermally grown oxide/Cr/Au and Cr/Au/Sn/Au metallization schemes described in Figure 5-7b were bonded at 340 °C for 2 min using the vacuum film bonding system. The temperature was ramped up and down at a rate of 40 °C/min. 30 psi of static pressure was applied during bonding. The bonded test coupons could not be pulled apart using tweezers. A diamond scribe was used to cleave the bonded sample successfully without the bonded test coupons separating.

This result was promising, as it implied that thinner layers of Au and Sn than that suggested in [18] were sufficient for forming a robust bond between test coupons, and the metallization scheme could possibly be translated to an optopill-to-recess bonding application. However, this metallization scheme still did not account for the need of good electrical conductivity between the optopill and the Si substrate. The need for a thermally grown oxide layer as a diffusion barrier for the Cr/Au metallization also implied the need for additional processing steps during either pill production or recess formation. It may also be difficult to implement the oxide layer without affecting actual device functionality when the optopill is an actual heterostructure device and the substrate an integrated circuit. Due to time constraints and the factors listed above, this metallization scheme was not further explored.

5.4. GaAs to Pd/Sn/Pd and GaAs to Al/Pd/Sn/Pd

Pd has been used for low temperature (30 min @ 350 °C) bonding of III-V semiconductors such as InP to GaAs substrates [27], [28]. This bonding mechanism

involves a solid-phase-topotaxial reaction between GaAs and Pd to produce Pd_4GaAs. In particular, work had been done by W.P. Giziewicz to bond arrays of GaAs pillars to flat substrates coated with a Pd/Sn/Pd stack [24]. Some measure of success had been obtained in this study when the bonding was carried out at 365 °C for 80 min. Glass slides were used to apply pressure to the pillared substrate and flat substrates. These 4 μm tall pillars had a 50 μm x 50 μm bonding surface. A brief study was done to see if optopills could be bonded to recesses using this GaAs to Pd/Sn/Pd bonding structure. An added benefit of this structure was that the Pd/Sn layers could also provide a relatively low resistance ohmic contact to n-GaAs. Contact resistivities of the order of 10^{-5} Ω cm^2 had been obtained by annealing Pd/Sn (300/1500 Å) contacts on n-GaAs [29].

Attempts were therefore made to bond bare n-GaAs pills to Pd/Sn/Pd pads in dummy recesses. The bare n-GaAs pills were approximately 40 μm in diameter and 5 μm tall. The Pd/Sn/Pd layers were deposited by W. P. Giziewicz on the dummy recesses using a thermal evaporator and patterned using lift-off lithography. The thicknesses of the layers were 0.100, 0.050 and 0.100 μm respectively. The recessed substrates were solvent cleaned immediately before the n-GaAs pills were placed in the recesses using vacuum tool MPAP. A bonding temperature of 365 °C and a bonding pressure of 10 psi were used. The temperature was ramped up and down at a 40 °C/min rate. Bonding time was varied. All bonding experiments were conducted using the vacuum film bonding apparatus.

The results of the bonding experiments done using the GaAs to Pd/Sn/Pd scheme are summarized in Table 5-3. In addition to the solvent clean and top-lift and push probe tip tests, a scotch tape test was administered to some of the bonded samples. A piece of tape was placed over the bonded sample and lifted off to see if the pills came off from the recessed substrate. It was obvious from the results of both bonding experiments that there were adhesion problems between Pd and Si, as the Pd/Sn/Pd pads were coming unattached from the recesses during bonding, solvent clean and the scotch tape test. Due to this issue, it could not be determined if the variation in bonding time had a significant effect on the bond quality. It was however encouraging that the Pd/Sn/Pd pads were still attached to the pills that had survived the probe tip top-lift and push-tests after they had been lifted off onto the tape.

Sample No.	Initial no. of pills placed in recesses	Bonding Temp. (°C)	Bonding Time (min)	Bonding Pressure (psi)	No. of pills left in place after solvent clean	No. of pills broken or left in place after top-lift and push tests (i.e. good bond)	Additional Notes
1	8	365	90	10	8	6	After the solvent clean, Pd/Sn/Pd pads were absent from some of the recesses. A scotch tape test removed all the remaining 6 pills along with the Pd/Sn/Pd pads from the recesses. The scotch tape was examined under the microscope, and it was observed that the pills that were removed still had the Pd/Sn/Pd pads attached to them.
2	5	365	60	10	5	3	After bonding, Pd/Sn/Pd pads were absent from some of the recesses even before the solvent clean. A scotch tape test removed the remaining 3 pills and all the Pd/Sn/Pd pads from the recesses.

Table 5-3 Summary of results of bonding bare n-GaAs optopills to Pd/Sn/Pd (0.1/0.05/0.1 μm) pads deposited in dummy recesses. The optopills were placed using vacuum tool MPAP and all bonding was done using the vacuum film bonding apparatus. Bonding temperature was ramped up and down at a 40 °C/min rate.

A 0.2 μm Al layer was introduced between the Pd/Sn/Pd pads and the Si surface of the dummy recesses to improve adhesion of the metal pads and the Si. The Al layer would also provide an ohmic contact to the underlying Si substrate. The Al/Pd/Sn/Pd (0.2/0.1/0.05/0.1 μm) pads were deposited and patterned in the dummy recesses using the e-beam and lift-off lithography processes listed in Appendix B.

One bonding run was done using this metallization scheme. 10 pills were placed by vacuum tool MPAP in the recesses and bonded at 370 °C for 90 min. A 40 °C/min ramp rate was used. The vacuum film bonding technique was used to apply 20 psi of pressure during bonding. There was definitely an improvement in the adhesion between the metal pad and the recess, as no pads fell out during any step of the bonding experiment. However, only 1 pill remained in place in a dummy recess after bonding. The other 9 pills were found attached to the vacuum film instead, possibly due to electrostatic attraction between the GaAs pills and the vacuum film. The remaining pill fell out during the solvent clean. It appeared that no bonding had actually occurred between the pills and the pads in the recesses. Due to the lack of additional bare GaAs pills and time constraints, no further experiments could be done using this metallization scheme.

5.5. Au to Ti/AuSn

Some success had been achieved in using the preformed AuSn eutectic solder to bond optopills to recesses using the metallurgical scheme described in Section 5.2., so further work was attempted using the AuSn perform. This time, instead of depositing the AuSn on the optopills, the AuSn layer was deposited in the recesses. Such a configuration would improve the ease of cleaning of the AuSn layer to remove oxides due to oxidation of the AuSn, if necessary.

Ti/AuSn (0.02/0.3 μm) pads were deposited and patterned in dummy recesses. The Ti served as an adhesion layer between the Si and AuSn. A Cr/Au/Ni/Au/Cr (0.04/0.1/0.25/0.1/0.01 μm) stack was sputtered onto dummy GaAs optopills. The first Cr/Au layer was to serve as an ohmic contact to the GaAs, and the Ni layer was included as a diffusion barrier between the two Au layers and so that the pills could be used for MASA as well. The outer Au layer was used as a wetting surface for the AuSn solder.

The outermost Cr layer was used to promote oxide mask adhesion during pill processing. Most, if not all, of the top Cr layer was sputtered off during a subsequent RIE processing step to remove the oxide mask. This was obvious in the change of coloration of the metal stack surface from a grayish tone (the typical appearance of a Cr layer) to a distinct yellow color characteristic of Au. This optopill structure is illustrated in Figure 3-1.

Sample No.	Initial no. of pills placed in recesses	Bonding Temp. (°C)	Bonding Time (min)	Bonding Pressure (psi)	No. of pills left in place after solvent clean	No. of pills broken or left in place after top-lift and push tests (i.e. good bond)
1	8	360	10	10	8	4
2	8	300	2	10	8	5

Table 5-4 Summary of results of bonding Cr/Au/Ni/Au (0.04/0.1/0.25/0.1μm) coated dummy optopills to Ti/AuSn (0.02/0.3 μm) pads deposited in dummy recesses. Bonding temperatures were ramped at a 40 °C/min rate.

Two bonding runs were done using this Cr/Au/Ni/Au to Ti/AuSn scheme. Vacuum tool MPAP and vacuum film bonding were used for pill placement and bonding respectively. The results of these runs are summarized in Table 5-4. The first sample was bonded at 360 °C for 10 min at 10 psi. Although half of the pills were removed from their recesses by the probe tip push test, it was found that there was still some residual Au left in 2 of these recesses after the pills were pushed off. There was a noticeable difference in coloration between these recesses and the recesses that were not filled with pills during bonding. SEM images of the recesses also showed a striated pattern in the previously filled recesses that was absent in the other empty recesses, while the AuSn solder was observed to ball up in the recesses that were not filled during bonding. This striated pattern was transferred from the optopills to the recess pads during bonding. This differential is illustrated by the SEM images in Figure 5-8a, b and c. Figure 5-8d is an SEM image of an optopill that passed the probe tip push test. Poor adhesion between the Cr/Au/Ni/Au stack and the GaAs optopills was thus suspected. This was confirmed by the fact that some of the pills had missing metal stacks even before they were etched free of their growth substrate. This is evident in Figure 5-9. This poor adhesion was most probably due to failure to perform a buffered oxide etch (BOE) of the GaAs material prior to metal deposition. Any oxide on the GaAs surface would affect metal adhesion.

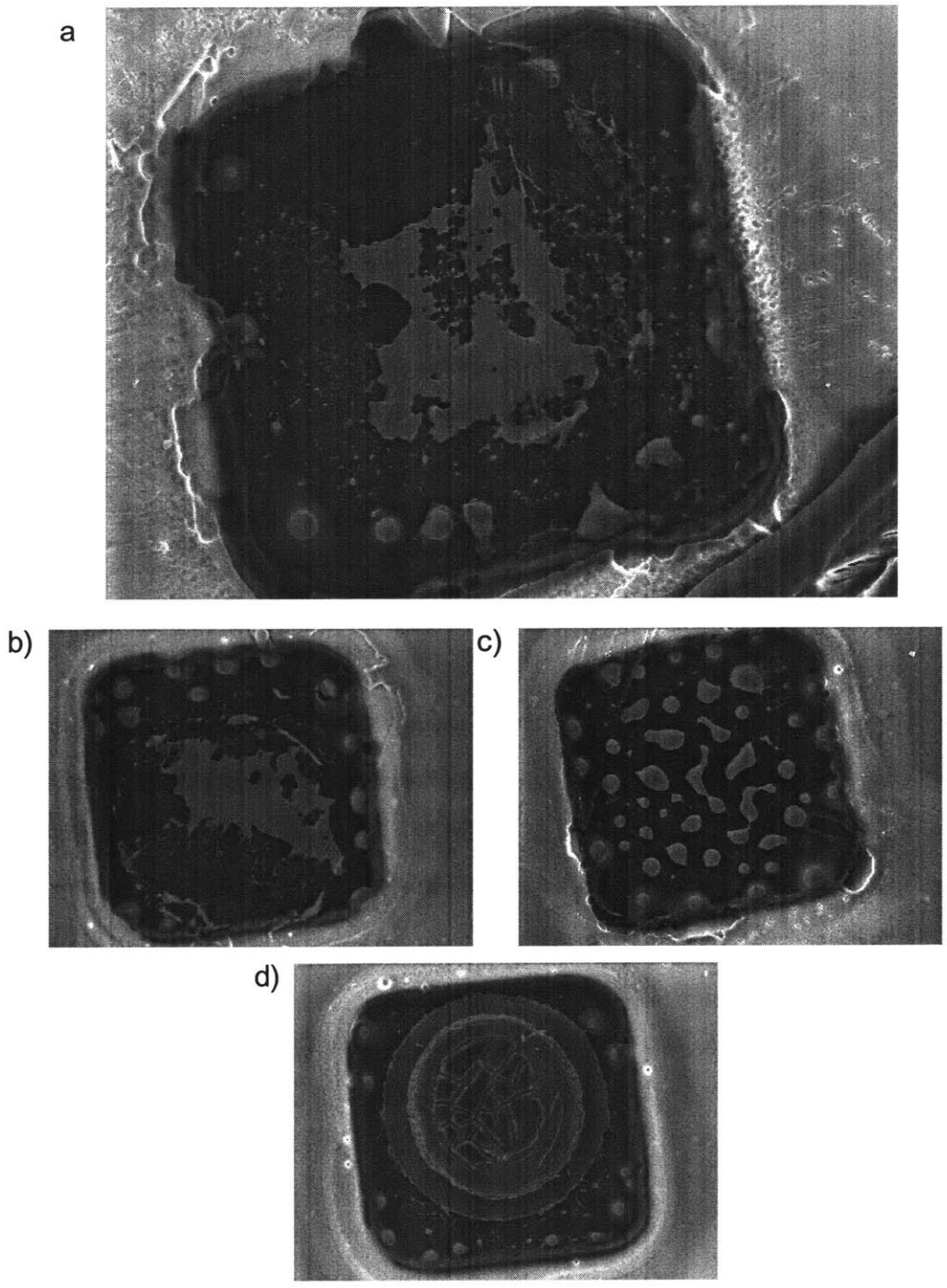

Figure 5-8 SEM images of sample no.1 listed in Table 5-4. Cr/Au/Ni/Au (0.04/0.1/0.25/0.1μm) coated dummy optopills were bonded to Ti/AuSn (0.02/0.3 μm) pads deposited in dummy recesses at 360 °C for 10 min using 10 psi of pressure. a) & b) Image of recesses from which bonded optopills had been removed using a probe tip. A striated pattern that was transferred from the optopill can be observed. c) Image of recess that was not filled with a pill during bonding. Balling of the AuSn solder due to the bonding temperatures can be observed. d) A successfully bonded optopill in a recess. The surface roughness on the top of the pill is due to residual AlAs from the etch stop layer that had oxidized.

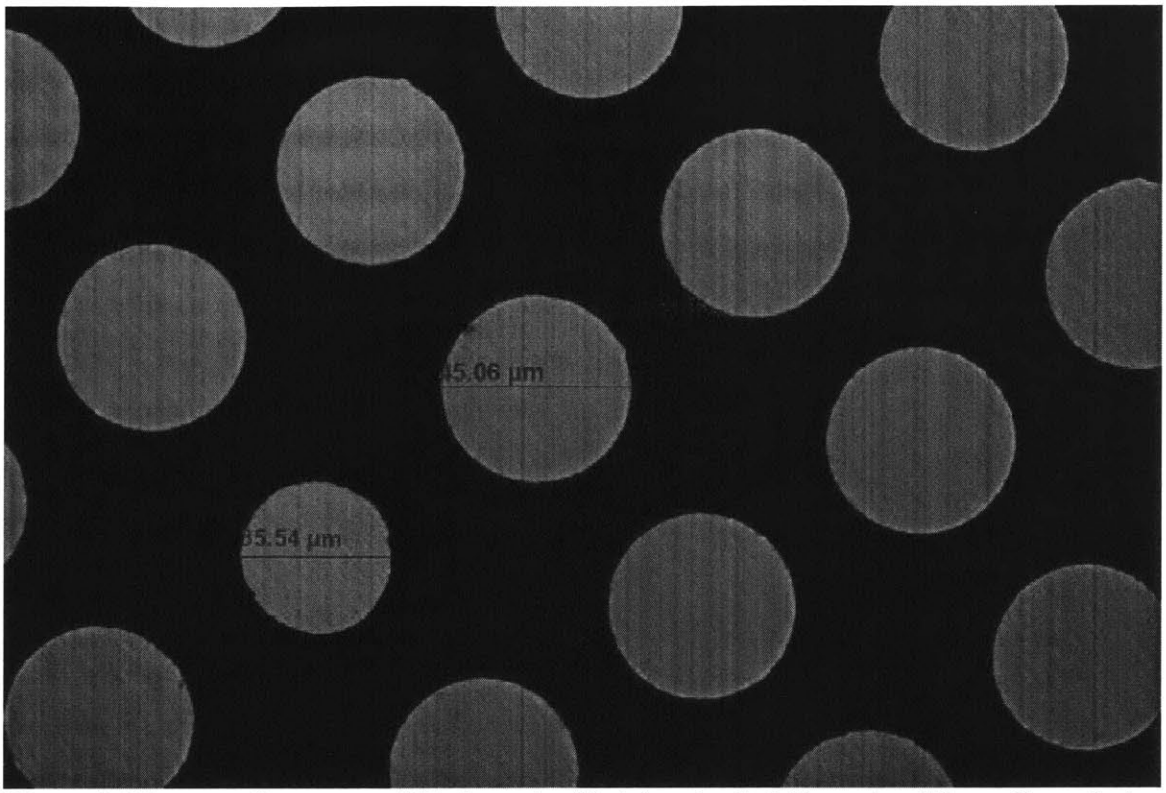

Figure 5-9 Image of an array of GaAs optopills taken by J. J. Rumpler. The yellow circles are the Cr/Au/Ni/Au/Cr metal stacks that had been sputtered on the optopills. The metal stack is missing from one of the optopills in this image. This optopill is identified by the smaller green circle. The discrepancy in the metal stack diameter and the GaAs diameter is due to lateral etching of the GaAs.

As 360 °C far exceeded the melting point of the AuSn preform, a lower bonding temperature, 300 °C, was attempted. The bonding time was also decreased to 2 min, as it was suggested that once the AuSn solder melted, it was only necessary to hold the bonding temperature for a brief period of time for the solder to wet the bonding surfaces for bonds to form. The bonding pressure was maintained at 10 psi. Out of 8 pills that were bonded in this second run, only 3 pills failed the probe tip push test. Some residual metallization from 2 of these pills were also left behind in their respective recesses. Figure 5-10a, b, and c are SEM images taken of this sample.

Taking into account the adhesion problem between the GaAs optopills and their metallization layers, the results of the two Au to Ti/AuSn bonding runs were promising. If the pills that had left residual metallization in the recess were considered to have a sufficiently good bond as well (since part of the Cr/Au/Ni/Au stack did adhere to the Ti/AuSn pads), the yield of both runs were at least 75 %. The use of the AuSn preform to

bond optopills to recesses was quite successful in this case. However, the Ti/AuSn layer did not form an ohmic contact with the underlying p-type Si. This led to the idea of including an Al layer in the metal stack deposited in the dummy recesses, while still using the AuSn preform for bond formation. This work is discussed in the next subsection.

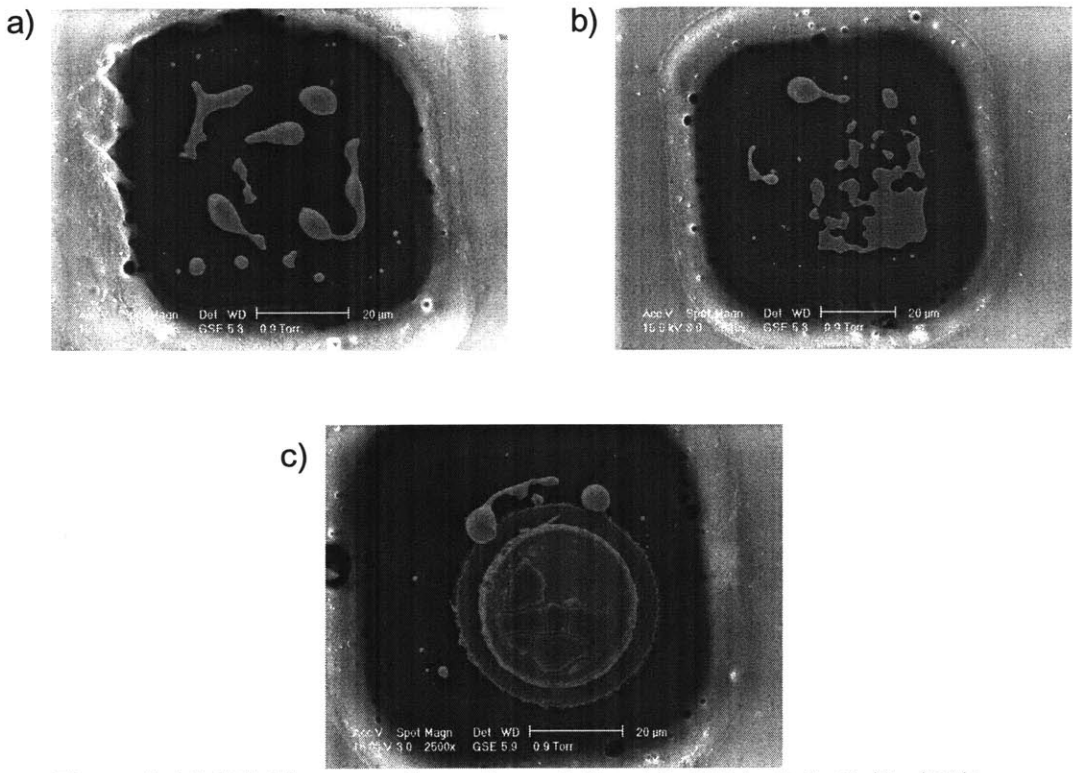

Figure 5-10 SEM images of sample no.2 listed in Table 5-4. Cr/Au/Ni/Au (0.04/0.1/0.25/0.1µm) coated dummy optopills were bonded to Ti/AuSn (0.02/0.3 µm) pads deposited in dummy recesses at 300 °C for 2 min using 10 psi of pressure. a) Image of recess that was not filled with a pill during bonding. Balling of the AuSn solder can be observed. b) Image of recesses from which bonded optopills had been removed using a probe tip. A striated pattern that was transferred from the optopill can be observed. c) A successfully bonded optopill in a recess. The surface roughness on the top of the pill is due to residual AlAs from the etch stop layer that had oxidized.

5.6. Au to Al/Pt/Au/AuSn and Au to Al/Pt/Au/AuSn/Au

The AuSn preform seemed to work fairly well as a bonding agent, but the AuSn bonding schemes discussed in the previous subsections failed to satisfy the need for electrical connectivity to the underlying Si substrate. An Al layer was therefore introduced to provide an ohmic contact to the underlying Si of the recessed substrate.

Since most of the optopill III-V monolithic integration will be done on Si IC chips, a bonding metallization that can both produce a robust bond and an ohmic contact to Si is highly desired.

Al/Pt/Au/AuSn pads were deposited in dummy recesses on highly doped (> 10^{19}), low resistivity p-type Si. Pt has been used as a diffusion barrier between Al and Au layers [30]. It was uncertain if Pt was a suitable diffusion barrier between Al and AuSn, so the Pt/Au layers were included between the Al and AuSn layers to prevent interdiffusion of Al and AuSn. The thicknesses of the Al, Pt, Au and AuSn layers were 0.100, 0.050, 0.020, and 0.200 μm respectively. The Cr/Au/Ni/Au (0.04/0.1/0.25/0.1μm) dummy GaAs optopills used in the bonding experiments for this metallization scheme are similar to those described in the Section 5.5., and their structure is shown in Figure 3-1.

5.6.1. Resistance Measurements

Some of these dummy recesses on a single Si chip were probed from pad to pad to determine if an ohmic contact was formed to the Si. Adjacent recesses were 200 μm apart, and the distance between the recesses furthest apart that were probed was approximately 800 μm. The resistances measured were approximately 5.4 Ω, regardless of the distance between the pads being probed. This, along with the low 0.01-0.02 Ω cm^2 resistivity of the Si substrate, was indicative that contact resistance was the main reason for the high readings. Nevertheless, straight line I-V curves were obtained, and the contacts were ohmic.

Several sets of dummy recesses with the Al/Pt/Au/AuSn pads were annealed to see if annealing would reduce the contact resistance. The first set was annealed at 300 °C for 4 min to simulate bonding conditions used previously for AuSn bonding. This was done to determine if the contact resistance, and thus the pad-to-pad resistance readings, could be lowered significantly during optopill-to-recess bonding alone. This sample was probed pad-to-pad and the resistances measured ranged from 3.68 Ω to 4.96 Ω. The contacts were ohmic, and the resistance measurements were slightly reduced compared to the pre-anneal sample readings.

Typically, Al contacts to Si are sintered at 400 to 450 °C for 30 to 60 min to ensure that the native Si oxide is reduced by the Al and there is good physical contact between the Al and Si [31]. At these sintering temperatures, however, AuSn would melt and ball up and result in a rough, highly uneven bonding surface. Thus, instead of depositing the Al/Pt/Au/AuSn pads in a single vacuum cycle. The Al/Pt/Au layers were deposited first. The dummy recesses with the Al/Pt/Au metallization were then sintered in an anneal furnace for 30 min at 400 °C. The PECVD deposited SiO_2 (that the recesses were patterned in) cracked during sintering and the sample could not be processed further to deposit the AuSn layer. The Al/Pt/Au metal pads were still intact, however, and the recesses were probed from pad to pad. There was no improvement in the contact resistance. In fact, the resistance values measured increased to the range of 7.27 Ω to 9.23 Ω. This could be due to the phenomenon of Al spiking in the Si. This often occurs during sintering due to the high solubility of Si in Al (0.5 atomic percent at 400 °C).

Sample Description	**Range of resistances measured between pads that were 200 μm to 800 μm apart (Ω)**
Pre-annealed sample: no annealing was done.	5.37 – 5.39
Sample annealed at 300 °C for 4 min	3.68 – 4.96
Sample sintered at 400 °C for 30 min. The Al/Pt/Au metallization was deposited before sintering. The AuSn top layer was to be deposited after sintering, but due to cracking of the silicon oxide that the recesses were patterned in, this final layer was not deposited before measurements were taken.	7.27 – 9.23

Table 5-5 Summary of results of pad-to-pad resistance measurements of Al/Pt/Au/AuSn pads in dummy recesses on highly doped (> 10^{19}), low resistivity (0.01-0.02 Ω cm^2) Si.

A barrier layer like TiN may be included between the Al and Si to alleviate this problem. This option was, however, not explored due to time constraints, as the priority of this study was to determine a suitable optopill-to-recess bonding technique. Moreover, Si CMOS technology is highly developed and Al contacts to Si have been well studied. Determining a suitable diffusion barrier to place between Al and Si would not be difficult.

If the Al/Pt/Au/AuSn or a similar metallization was suitable for bond formation, the diffusion barrier could be included before the Al layer to improve contact resistance.

The resistance measurements of the various samples tested are summarized in Table 5-5.

5.6.2. Bonding

Flat substrate to flat substrate bonding was first attempted using the Al/Pt/Au/AuSn metallization. Cr/Au/Cr (0.04/0.1/0.01 μm) was deposited on a flat Si substrate. The 40 nm thick Cr layer was used to promote Au to Si adhesion. The Au layer simulated the top Au surface of the optopills, and the outermost 10 nm thick Cr layer was included to see would affect bond formation. This was due to concerns of the effects on bonding if the Cr layer was not completely sputtered off during RIE processing of the pills, and if a wet etch of this top Cr layer should be incorporated to pill processing. Two pairs of 5 mm x 5 mm test coupons were bonded using these metal layers. The first sample was bonded at 340 °C and 10 psi for 5 min with a temperature ramp rate of 50 °C/min. The second sample was bonded at 340 °C and 20 psi for 10 min with the same temperature ramp rate. Both pairs of test coupons did not adhere to each other at all and were separated when lifting off the heating strip after annealing. The Cr/Au/Cr surfaces did show any signs of AuSn wetting. These results indicate that a clean, complete removal of the top Cr layer on the optopills is necessary for bond formation.

An Al/Pt/Au coated Si test coupon was sintered at 400 °C before a final AuSn layer was deposited on it. The surface of the sintered sample was noticeably rough. The sintered Al/Pt/Au/AuSn test coupon was bonded to a Cr/Au (0.04/0.1 μm) coated test coupon at 340 °C and 10 psi for 5 min. The test coupons were stuck together but easily pulled apart with a pair of tweezers. AuSn wetting of the Au bonding surface was observed. Surface roughness due to the pre-bonding sinter most probably hindered the formation of a stronger bond. This result meant that sintering or annealing of the Al/Pt/Au/AuSn sample before bonding was not recommended, so this was not done in the rest of the experiments discussed here.

There were also concerns that the AuSn bonding mechanism was more sensitive to bonding temperature than previously assumed in this study, and that the bonding temperature should kept within closer range to the melting point of the AuSn solder. An Al/Pt/Au/AuSn sample was thus heated in the vacuum film bonding apparatus (the vacuum film was removed since pressure application was not required) and observed to determine the thermocouple reading corresponding to the 282 °C melting point of AuSn. This heating run was also done within a day of the AuSn deposition. Some slight discrepancy of a few degrees between the thermocouple reading and the actual sample temperature was expected due to heat transfer losses. This sample was heated up to 400 °C and there was still no signs of the AuSn melting. This was unexpected since the AuSn had shown signs of melting (wetting of the Au bonding surface) at 340 °C in the previous bonding experiments. There was reason to suspect that there was something wrong with the AuSn deposition.

Another sample that had been coated with the Al/Pt/Au/AuSn stack in a separate deposition run was heated up in the same manner. This sample will be referred to as Sample A in the next few paragraphs. The AuSn layer of this sample was observed to melt at 290 °C, and the AuSn liquid lake was observed to spread smoothly from one corner over the entire 5 mm x 5 mm surface within 30 s. This heating run was also done within a day of the AuSn deposition.

The failure of the AuSn layer on the previous sample to melt suggests that it would be useful, for future purposes, to run a flat Si piece along with the substrate recesses during each metal deposition run. This flat Si piece could be used for calibration purposes. It should be used to determine the thermocouple reading at melting point of the AuSn solder and to ensure that there are no problems with the AuSn layer such as the faulty deposition run mentioned here.

A flat Si test coupon that had been in the same metal deposition run as Sample A was bonded to a Cr/Au (0.04/0.1 μm) coated Si test coupon at 290 °C and 10psi for 4 min. It was found that the 2 test coupons could not be pulled apart using tweezers.

Optopill to flat substrate bonding was attempted using another flat substrate that had been processed in the same deposition run as Sample A. This was done a week after the deposition. The flat substrate was solvent cleaned before 8 Cr/Au/Ni/Au coated optopills were placed using vacuum tool MPAP. Bonding was done at 290 °C and 10 psi for 4 min. After bonding, only 7 optopills remained in place on the flat substrate. No more pills were lost during a solvent clean. A micropipette was used to try to pick up the pills. None of these pills were lifted off by vacuum tool MPAP. However, 4 of these pills were dislodged when the micropipette was used to push at the side of the pills, and 2 more were pushed off with some effort using a probe tip. The III-V material of the last pill was pushed off, but it left behind a ring of metal that was still stuck to the flat substrate, indicating a good bond. This last observation is not unexpected considering the optopill metal-to-semiconductor adhesion issues discussed earlier in Section 5.5.. Nevertheless, the yield rate of this run was very poor. The time differential between the metal deposition and the optopill placement led to the inference that significant oxidation of the AuSn solder may have occurred and prevented quality bond formation.

An Al/Pt/Au/AuSn flat substrate from the same deposition run as Sample A was thus heated up 2 weeks after metal deposition to observe for differences in the AuSn behavior such as melting point. This substrate was found to also melt at 290 °C. However, the liquid lake spread over the sample in a slower and more sporadic pattern. Instead of a single liquid lake spreading smoothly from one corner of the sample over the entire sample, spreading patches of small liquid lakes were observed to form simultaneously over the surface. After 1 min, the liquid lakes still did not cover the entire surface, and there was a slight difference in coloration between these patches and the parts of the surface that were not covered by the liquid lakes. This discrepancy compared with the behavior of the AuSn layer in Sample A was attributed to oxidation of the AuSn that had occurred over the 2 weeks between the two heating runs.

It was evident that the oxidation of the top AuSn layer would have to be removed in order to promote good bonding. Gary Trott from Agilent Laboratories suggested using a H_2O, HF and HNO_3 10:1:1 etch clean solution that was discussed in [32]. In order to eliminate the need for this etch clean step, a 10 nm top layer of Au was used instead to

prevent oxidation of the underlying AuSn layer. This Al/Pt/Au/AuSn/Au (0.1/0.05/0.02/0.2/0.01 μm) stack was deposited in a single vacuum cycle. This metallization scheme is illustrated in Figure 5-11. A flat substrate with this metallization was heated up to observe if the additional Au layer would affect the spread of the AuSn solder during melting. A liquid lake was observed to form at 290 °C and spread smoothly across the surface within 30 s. These observations corresponded to that obtained for Sample A, so the additional Au layer did not appear to have a significant effect on the spread of the AuSn solder and its melting point.

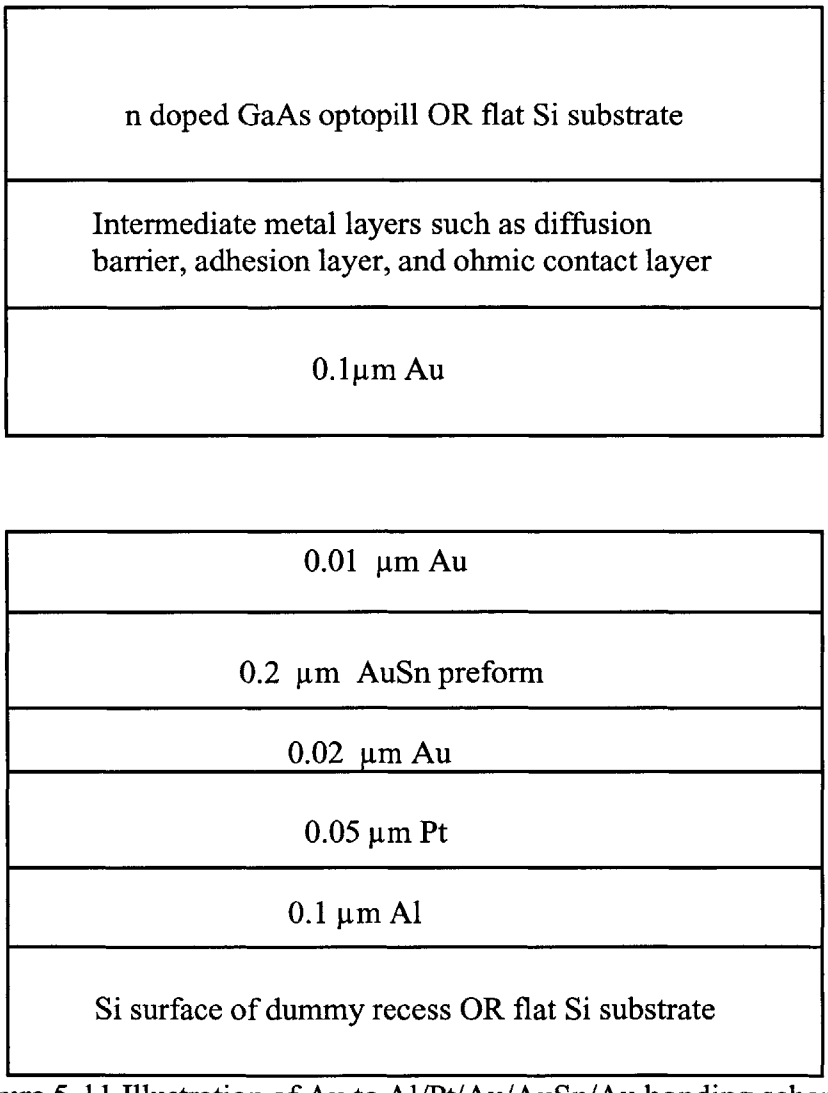

Figure 5-11 Illustration of Au to Al/Pt/Au/AuSn/Au bonding scheme.

An Al/Pt/Au/AuSn/Au coated flat Si substrate was bonded to a Cr/Au coated flat Si substrate at 290 °C and 10 psi for 4 min. Both metal surfaces were solvent cleaned

immediately prior to bonding. The test coupons could not be pulled apart with tweezers. A razor blade was used to pry the two test coupons apart. While the Si test coupons did not break into pieces (Si is much less brittle than III-V material like GaAs and InP), the Cr/Au test coupon did leave small residual bits of Si on the Al/Pt/Au/AuSn test coupon. The bond was strong enough that the edges of the Si test coupon had chipped during bonding.

A new set of dummy optopills with the same Cr/Au/Ni/Au metallization as those previously used was processed by J.J. Rumpler. This time, a BOE was done before metal deposition on the pills to eliminate the adhesion issue between the semiconductor and metal layers that was due to oxide formation on the semiconductor surface. As before, a thin layer of approximately 10 nm of Cr was deposited on the outer Au layer to promote oxide mask adhesion during pill processing. The Cr/Au/Ni/Au/Cr metal stack had a grayish coloration due to the top Cr layer. After an RIE etching step during pill processing, this outermost Cr layer was sputtered off to reveal the yellow Au layer beneath it. The amount of Cr that was left, if any, on the Au bonding surface, was negligible. After the metal layers were sputtered on, the optopills were rapidly annealed at 400 °C for 12 s to promote ohmic contact formation between the innermost Cr/Au layers and the GaAs material of the optopill.

Unfortunately, there were problems with the cleanliness and quality of this new batch of pills that were dispensed for vacuum tool placement and bonding. Many of the dispensed pills were coated with a layer of residue regardless of their orientation on the glass slide. This is pictured in Figure 5-12. This residue was possibly due to the polymer that was used to hold the pills in place during the back-side etch to etch them free of their growth substrate. Previous batches of pills which did not have this residue problem had been held in Apezion wax during the back-side etch instead of the polymer. It should also be noted that there were suspicions of a poorly grown AlAs etch-stop layer as some of the pills were etched completely during the back-side etch, with only the metal stacks remaining on the polymer.

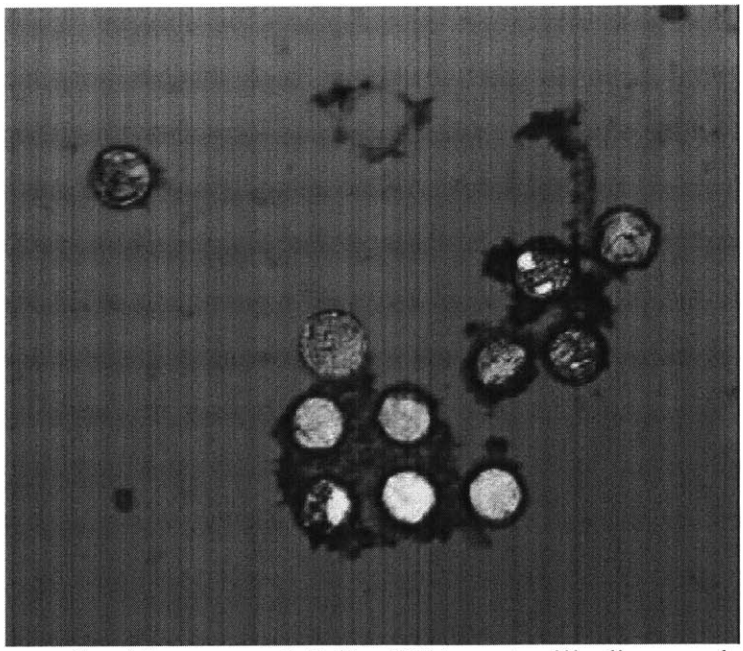

Figure 5-12 Image of residue covered Cr/Au/Ni/Au optopills dispensed on a glass slide. The gold colored pills are oriented with the metal side up and the silvery colored pills are oriented with the metal side down. The latter pills were selected for MPAP. Most of the pills are covered or surrounded with a fuzzy residue regardless of their orientation.

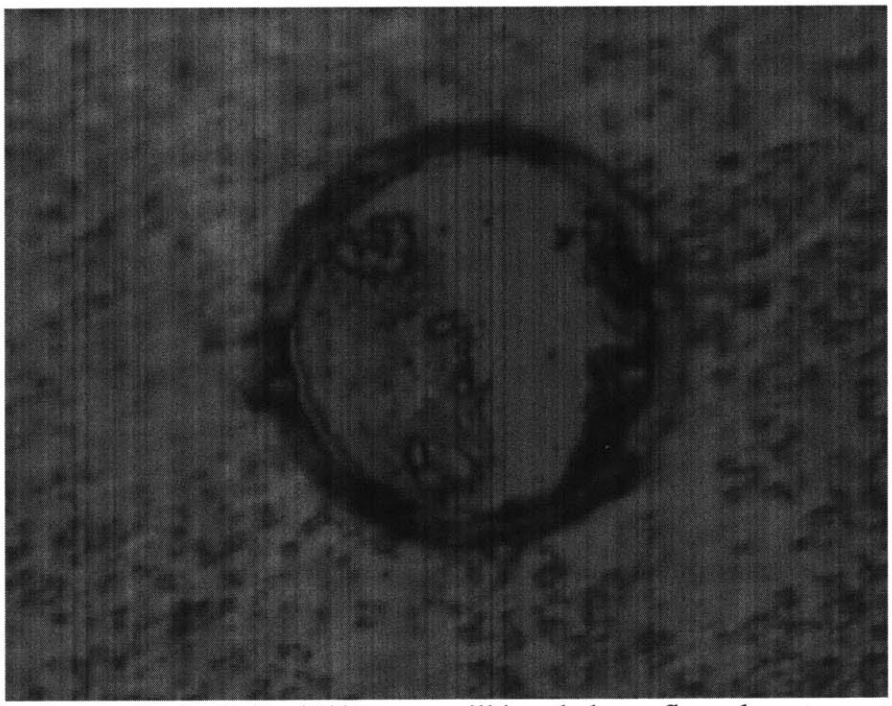

Figure 5-13 Image of a Cr/Au/Ni/Au optopill bonded to a flat substrate coated with Al/Pt/Au/AuSn/Au. As can be observed of the right edge of this pill, parts of the GaAs pill were broken off when a micropipette tip was used to attempt to dislodge the pill. The pill did not budge after repeated pushing at it with the micropipette tip. The quartz micropipette tip finally broke during one of these attempts to push the pill out of place.

Some of these pills were nonetheless placed on solvent cleaned flat substrates coated with Al/Pt/Au/AuSn/Au and two attempts were made to bond them at 290 °C and 15 psi for 4 min. Of the 6 pills that were placed and bonded on the first sample, 5 of them could be pushed out using a micropipette. The last pill, however, could not be picked up or pushed out using a micropipette. Parts of the pill edge broke off during repeated attempts to push the pill off. This pill is shown in Figure 5-13. Finally, the quartz micropipette tip broke in the last attempt to dislodge the pill. This result is promising as the resultant bond was stronger than the GaAs pill material. The failure of the other 5 pills to bond could be due to the residue that was surrounding the pills. This residue may have been present on the underside of the pills. Having this residue between the two bonding surfaces would definitely prevent quality bond formation.

The second sample produced similar results. Of the 6 pills placed and bonded, all stayed in place during a solvent clean and could not be picked up using vacuum tool MPAP. However, 4 of the pills could be nudged out of place by pushing on the side using a probe tip. As discussed previously, this could be due to the presence of the residue (from the pills) between the bonding surfaces.

Some of the dummy optopills from the same residue-ridden batch were placed on Al/Pt/Au/AuSn/Au pads in dummy recesses. The dummy recesses were solvent cleaned before pill placement. This sample was bonded at 290 °C and 15 psi for 4 min. Of the 8 pills placed, 3 fell out during a solvent clean after bonding. The remaining 5 pills could not be picked up by vacuum tool MPAP, but only 1 of them was not pushed off from the side using a probe tip. Residue from the pills was again suspected to be the reason for the weak bonds.

Due to time constraints compounded by the lack of cleaner optopills, no further bonding experiments were done with the Au pill to Al/Pt/Au/AuSn/Au metallization scheme. The results obtained so far with the AuSn preform solder seem promising and further work should be done using this metallization if and when cleaner optopills are obtained. The metallization scheme is the most practical of those discussed here since the Al layer forms an ohmic contact to Si. This ohmic contact could be further improved by

adding a diffusion barrier between the Al and Si to prevent Al spiking. With clean optopills, it is expected that the yield rate of good quality bonds between the Cr/Au/Ni/Au optopills and Al/Pt/Au/AuSn/Au pads in recesses will be greatly improved.

Chapter 6

Conclusions and Future Work

6.1. Conclusions

Two aspects of RM^3 optopill integration technology, namely optopill assembly and optopill-to-recess bonding, were the focus of this study. Significant strides were taken towards developing this technology for integrating III-V optoelectronic devices on Si IC chips. Firstly, a vacuum-tool MPAP technology for assembling III-V device optopills onto recessed Si substrates was developed successfully. An optimum design for the micropipette vacuum tool was determined and cleaning and storage procedures for the micropipettes were defined.

In addition, a vacuum film bonding technique was designed to apply uniform static pressure on samples during optopill-to-recess bonding. This technique overcame the issues of irregular pill height and recess depth that hindered previous pressure application techniques, and provided a straightforward means to measure bonding pressure. Progress was also made in determining a suitable metallization scheme for bonding optopills to their target recesses. Several metallization schemes were investigated and ruled out, while several bonding structures using the AuSn eutectic preform were found to be the most suitable for low-temperature bonding of the optopills. The effect of the oxidation of AuSn on bonding was investigated and the need for an Au protective layer was determined. An Al layer was also included for ohmic contact formation to Si in the last two metallization schemes studied. The Au optopill to Al/Pt/Au/AuSn/Au recess pad metallization scheme was thus determined to be the most promising for optopill bonding,

although time constraints and limited optopill availability prevented more bonding experiments using this bonding scheme. This scheme is summarized in Figure 6-1.

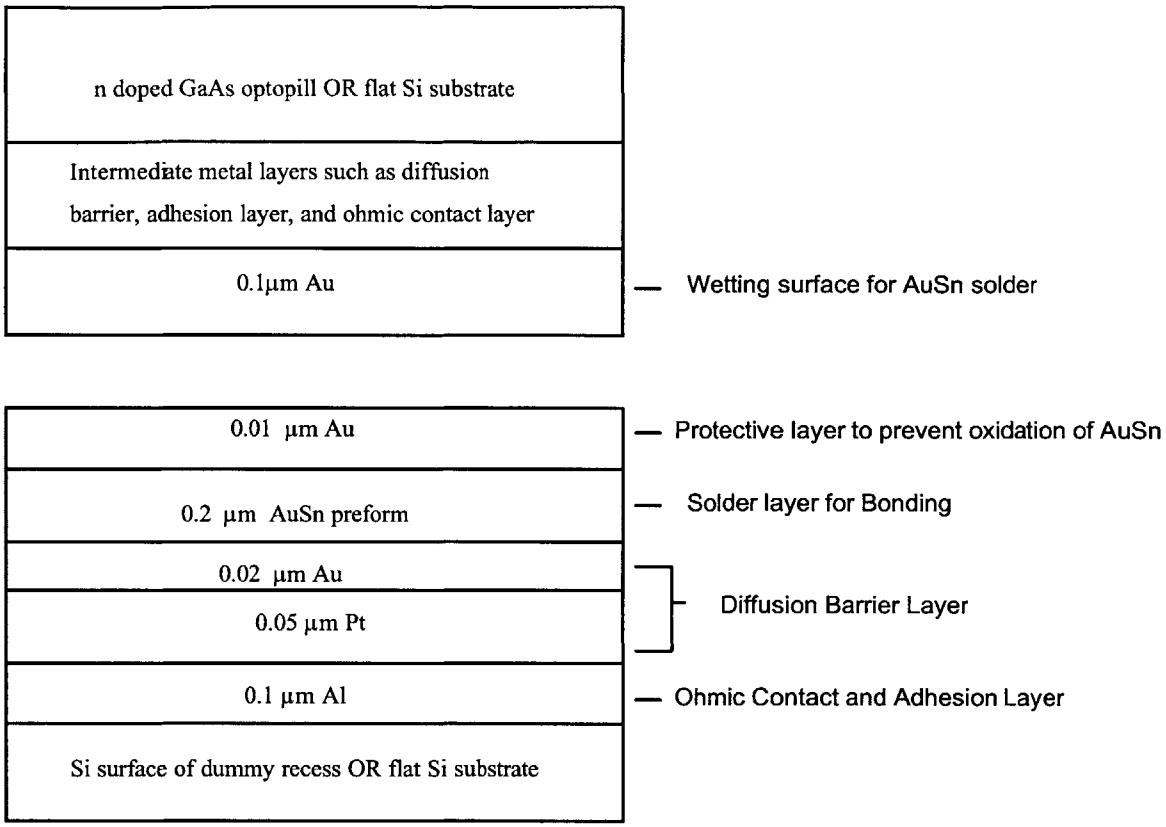

Figure 6-1 Schematic summarizing the Au to Al/Pt/Au/AuSn/Au bonding scheme and the function of each layer of metallization.

6.2. Future Work

Current vacuum-tool MPAP technology requires manual control and is quite tedious and impractical for large volumes of pill assembly. Ultimately, the solution lies in automating the vacuum-tool MPAP technology while maintaining the vacuum pick-up principles. An alternate vacuum tool design for such an application was suggested in this thesis. Future work should be done to incorporate the capabilities of MPAP, such as multiple device type assembly, with the benefits of high-speed automation.

Further investigation into suitable metallization structures for optopill-to-recess bonding must also be conducted. In particular, the Au to Al/Pt/Au/AuSn/Au bonding scheme should be further studied using clean, residue-free optopills. Further work should also look into reducing contact resistance and perhaps modifying the first few layers of

the Al/Pt/Au/AuSn/Au structure to eliminate issues like Al spiking. For instance, a barrier could be added between the Si recesses and Al. Reliable optopill-to-recess bonding is fundamental to the success of RM^3 technology.

Once the bonding technology is perfected, fully functional monolithically integrated circuits can be processed. Production efficiency will be greatly improved once MPAP is automated and capable of large scale pill assembly. Together, these techniques will prove RM^3 technology to be a valuable technology for monolithic heterogeneous integration.

Appendix A

Micropipette Recipes

The cleaning and storage procedures for the quartz micropipettes used in vacuum tool MPAP are summarized as follows.

A.1. Micropipette Cleaning Recipe

Step No.	Cleaning Step Description
1	Ultrasonication in acetone for 10 min at 40 kHz
2	Methanol and isopropanol clean using squirt bottles
3	Blow dry with nitrogen air gun

Table A-1 Micropipette Cleaning Recipe

A.2. Micropipette Storage

The micropipettes should be stored as suggested below:

a) Static dissipative case in desiccator cabinet

OR

b) Static dissipative case in two layers of ziplock bags with a packet of desiccant between the two bags. The desiccant packet should never be in direct contact with the case.

Appendix B

Processing Recipes

The following recipes were used to process dummy recesses on pieces of Si. All equipment used, unless otherwise mentioned, was located in EML, MIT.

B.1. Silicon Oxide Deposition

1. Solvent clean (acetone, methanol, IPA) and blow dry

2. Plasmatherm PECVD

   i. Chamber clean (no sample in chamber)

   Gas Flow: 300 sccm CF_4/O_2
   Pressure: 300 mTorr
   Temperature: 150 °C
   Power: 300 W
   Time: 30 min

   ii. Pre-deposition Run (no sample in chamber)

   Gas Flow: 600 sccm SiH_4, 300 sccm N_2O
   Pressure: 500 mTorr
   Temperature: 250 °C
   Power: 25 W
   Time: 5 min

   iii. SiO_2 Deposition (sample in chamber)

   Gas Flow: 600 sccm SiH_4, 300 sccm N_2O

Pressure: 500 mTorr
Temperature: 250 °C
Power: 25 W
Rate: ~ 30 nm/min

iv. Chamber clean (no sample in chamber)

Gas Flow: 300 sccm CF_4/O_2
Pressure: 300 mTorr
Temperature: 150 °C
Power: 300 W
Time: 20 min and additional 30 min per micron of film deposited

v. De-fluorination --- RF Purge (no sample in chamber)

Pressure: 800 mTorr
Power: 200 W
Time: 5 min

Note: For thick depositions, the clean and pre-deposition steps were repeated after every 2 μm of deposition. The chamber also had to be cleaned after the deposition was done and the sample had been taken out.

B.2. Thick Resist Photolithography for Recesses

1. Solvent clean (acetone, methanol, IPA) and blow dry
2. Dehydration bake, 10 min @ 130 °C
3. HMDS spin on (coater), 30 s @ 4 krpm
4. Bake, 10 min @ 130 °C
5. Thick Resist (AZ 4620) spin on (coater), ~ 10 μm
   i. 9 s @ 1.5 krpm
   ii. 60 s @ 1 krpm
   iii. 10s @ 5 krpm
6. Softbake, 60 min @ 90 °C

7. Exposure (Karl Suss MJB-3 Aligner) with mask for 25 s
8. Develop in AZ 440 for 2 min
9. Postbake, 30 min @ 90 °C

B.3. Silicon Oxide Etch

1. Plasmatherm RIE
   i. Pre-etch Run (no sample in chamber)

      Gas Flow: 20 sccm HC14
      Pressure: 25 mTorr
      Temperature: 25 °C
      Power: 300 W
      Time: 5 min

   ii. Etch (sample in chamber)

      Gas Flow: 20 sccm HC14
      Pressure: 25 mTorr
      Temperature: 25 °C
      Power: 300 W
      Rate: ~ 60 nm/min

   iii. Chamber clean

      Gas Flow: 30 sccm O_2
      Pressure: 30 mTorr
      Temperature: 25 °C
      Power: 300 W
      Time: 10 min

B.4. Electron Beam Metal Stack Deposition in Recesses

1. Wet etch to remove residual oxide from recess surface
   i. 10 – 15 sec dip in BOE (buffered oxide etch)
2. E-beam Evaporator

i. Run pressures: 3 x 10^{-6} mTorr – 3 x 10^{-5} mTorr
Deposition Rate: 2 – 3 Å/s

B.5. Lift-off

1. Immerse sample in acetone and agitate until photoresist and unwanted metal is lifted off (1 to 2 min)

B.6. Image Reversal Photolithography for Ohmic Contacts

1. Solvent clean (acetone, methanol, IPA) and blow dry
2. Dehydration bake, 10 min @ 130 °C
3. HMDS spin on (coater), 30 s @ 4 krpm
4. Bake, 10 min @ 130 °C
5. Image Reversal Resist (AZ 5214) spin on (coater), ~ 2 μm
   i. 5 s @ 500 rpm
   ii. 30 s @ 2 krpm
6. Prebake, 20 min @ 90 °C
7. Exposure (Karl Suss MJB-3 Aligner) with mask for 5 s
8. Postbake, 20 min @ 90 °C
9. Flood Exposure (Karl Suss MJB-3 Aligner) without mask for 60 s
10. Develop in AZ 422 for 1-2 min

Note: The e-beam and lift-off recipes (B.4. and B.5.) were also used to deposit and lift off the ohmic contacts on the bonded pills in recesses. However, instead of thick resist photolithography, image reversal photolithography was used to pattern the ohmic contact rings.

Bibliography

[1] A.V. Krishnamoorthy, et al., "Vertical-Cavity Surface-Emitting Lasers Flip-Chip Bonded to Gigabit-per-Second CMOS Circuits," *IEEE Photonics Technology Letters,* vol. 11, no.1, pp.128-130, 1999.

[2] K. van der Zanden, et al., "Metamorphic In.53Ga.47As/ In.52Al.48As HEMT's on Germanium substrates," *IEEE Electron Device Letters*, vol. 21, no. 2, pp. 57-79, 2000.

[3] P. Bhattacharya, *Semiconductor Optoelectronic Devices*, Prentice-Hall, Inc., New Jersey, pp. 18, 1997.

[4] S. M. Sze, *Physics of Semiconductor Devices*, John Wiley & Sons, Inc., United States of America, pp. 848-850, 1981

[5] J. M. London, "Preparation of Silicon-on-Gallium Arsenide Wafers for Monolithic Optoelectronic Integration," *IEEE Photonics Technology Letters*, vol. 11, no. 8, pp. 958-960, 1999.

[6] P. Bhattacharya, *Semiconductor Optoelectronic Devices*, Prentice-Hall, Inc., New Jersey, pp. 486, 1997.

[7] U. Gösele, et al., "Wafer bonding: a flexible approach to materials integration," Conference Proceedings - International Conference on Indium Phosphide and Related Materials, pp. 231, 1999.

[8] U. Gösele, et al., "Wafer bonding for microsystems technologies," *Sensors and Actuators A: Physical*, vol. 74, no.1, pp. 161-168, 1999.

[9] J. E. Cunningham and W.Y. Yan, "Integration issues for 850 nm optical modulators on Si electronics by direct epitaxy," *Journal of Vacuum Science and Technology B: Microelectronics Processing and Phenomena*, vol. 15, no. 4, pp. 886-890, 1997.

[10] J. J. Talghader, "Integration of LEDs and VCSELs using fluidic self-assembly," *Proceedings of SPIE - The International Society for Optical Engineering*, vol. 3286, pp. 86-95, 1998.

[11] J. J. Talghader, J.K. Tu and J.S. Smith, "Integration of fluidically self-assembled optoelectronic devices using a silicon-based process," *IEEE Photonics Technology Letters*, vol. 7, no. 11, pp. 1321-1323, 1995.

[12] H. Wang, et al., "Monolithic Integration of SEED's and VLSI GaAs Circuits by Epitaxy on Electronics," *IEEE Photonics Technology Letters*, vol. 9, no. 5, pp. 607-609, 1997.

[13] W. P. Giziewicz and C. G. Fonstad Jr., "Optoelectronic integration using aligned metal-to-semiconductor bonding," *Journal of Vacuum Science and Technology, Part A: Vacuum, Surfaces and Films*, vol. 20, no. 3, pp. 1052-1056, 2002.

[14] C. G. Fonstad Jr., "Monolithic Integration of Optoelectronic Devices with VLSI Electronics --- using reduced-temperature epitaxy and bonding," *DOE Optical Interconnects for High Performance Computing Workshop*, 1999.

[15] J. J. Rumpler, "Optoelectronic Integration Using the Magnetically Assisted Statistical Assembly Technique: Initial Magnetic Characterization and Process Development," Master of Science Thesis, MIT EECS, September 2002.

[16] J. M. Perkins, "Magnetically Assisted Statistical Assembly of III-V Heterostructures on Silicon: Initial Process and Technology Development," Master of Science Thesis, MIT EECS, May 2002.

[17] Precision Micro Devices, LLC, 45 Leveroni Ct. #201, Novato, CA 94949, ph. 415-884-0844, fax 415-884-0846, contact person: April Dean.

[18] G. R. Dohle, et al., "A New Bonding Technique for Microwave Devices," *IEEE Transactions on Components, Packaging, and Manufacturing Technology --- Part B*, vol. 19, no.1, pp. 57-63, 1996.

[19] G. R. Dohle, et al., "Low Temperature Bonding of Epitaxial Lift Off Devices with AuSn," *IEEE Transactions on Components, Packaging, and Manufacturing Technology --- Part B*, vol. 19, no. 3, pp. 575-580, 1996.

[20] C. C. Lee, C. Y. Wang and G. S. Matijasevic, "A New Bonding Technology Using Gold and Tin Multilayer Composite Structures," *IEEE Transactions on Components, Hybrids, and Manufacturing Technology*, vol. 14, no. 2, pp. 407-412, 1991.

[21] E. Zakel and H. Reichl, "Au-Sn Bonding Metallurgy of TAB Contacts and Its Influence on the Kirkendall Effect in the Ternary Cu-Au-Sn," *IEEE Transactions on Components, Hybrids, and Manufacturing Technology*, vol. 16, no. 3, pp. 323-332, 1993.

[22] I. H. Tan, et al., "Low-temperature Pd bonding of III-V semiconductors," *Electronic Letters*, vol. 31, no. 7, pp. 588-589, 1995.

[23] E. Yablonovitch, et al., "Van der Waals bonding of GaAs on Pd leads to a permanent, solid-phase-topotaxial, metallurgical bond," *Applied Physics Letters*, vol. 57, no. 24, pp. 3159-3161, 1991.

[24] W. P. Giziewicz, "Optoelectronic Integration using Aligned Metal-to-Semiconductor Bonding," Master of Engineering Thesis, MIT EECS, June 2000.

[25] Airtech Advanced Materials Group, 5700 Skylab Road, Huntington Beach, CA 92467, ph. 714-899-8100, fax 714-899-8179, http://www.airtechonline.com

[26] M. Hansen and K. Anderko, *Constitution of Binary Alloys*, McGraw-Hill Book Company, Inc., New York, 1958.

[27] I. -H. Tan, et al., "Low-temperature Pd bonding of III-V semiconductors," *Electronic Letters*, vol. 31, no. 7, pp. 588-589, 1995.

[28] E. Yablonovitch, et al., "Van der Waals bonding of GaAs on Pd leads to a permanent, solid-phase-topotaxial, metallurgical bond," *Applied Physics Letters*, vol. 59, no. 24, pp. 3159-3161, 1991.

[29] M. S. Islam, et al., "The importance of the Pd to Sn ratio and of annealing cycles on the performance of Pd/Sn ohmic contacts to n-GaAs," *Thin Solid Films*, vol. 292, pp. 264-269, 1997.

[30] C. –T. Lee, H. –W. Kao and F. –T. Hwang, "Effect of Pt Barrier on Thermal Stability of Ti/Al/Pt/Au in Ohmic Contact with Si-Implanted n-type GaN layers," *Journal of Electronic Materials*, vol. 30, no. 7, pp. 861-865, 2001.

[31] J. D. Plummer, M. D. Deal and P. B. Griffin, *Silicon VLSI Technology Fundamentals, Practice and Modeling*, Prentice Hall, Inc., New Jersey, 2000.

[32] R. R. Thompson, D. R. Cropper and B. W. Whitaker, "Bondability Problems Associated with the Ti-Pt-Au Metallization of Hybrid Microwave Thin Film Circuits," *IEEE Transactions on Components, Hybrids, and Manufacturing Technology*, vol. CHMT-4, no. 4, 1981.